REVIEW

CrossMark

Magnetic Fe$_3$O$_4$ based layered double hydroxides (LDHs) nanocomposites (Fe$_3$O$_4$/LDHs): recent review of progress in synthesis, properties and applications

Cheera Prasad[1] · Hua Tang[1] · Wei Liu[1]

Abstract

In view of the previous work on magnetic Fe$_3$O$_4$ nanoparticles-based layered double hydroxides (magnetic Fe$_3$O$_4$/LDHs) as novel photocatalyst, research on this group of composites became one of the most attractive topics of nowadays. The magnetic Fe$_3$O$_4$/LDHs materials are often utilized for environmental remediation and photocatalysis. Hybrids of layered double hydroxides (LDHs) and Fe$_3$O$_4$ MNPs are efficient nanocomposites due to their flexible properties and the excess of composition available for modification. So, critically reviews on the hybrid of the work magnetic Fe$_3$O$_4$/LDHs composite are the first report that efficient nanocomposites because of their flexible properties, energy and time used for separation, reduced consumption of additional materials can result in significant environmental and economic benefits. "The electrostatic interaction between the positively charged LDHs nanocomposites and negatively charged Fe$_3$O$_4$ MNPs is adequate to make the formation of stable self-assembly of the two components". This review article discussed the magnetic Fe$_3$O$_4$/LDHs nanocomposites synthesis and applications in the photo catalysis, drug delivery and environmental remediation.

Keywords Magnetic Fe$_3$O$_4$NPs · LDHs nanocomposite · Fe$_3$O$_4$/LDHs nanocomposites

Introduction

At present, the preparation of magnetic nanoparticles (MNPs) consciously studied owing to their great fundamental scientific attention as well as many technological applications in water purification and photocatalysis [1–4]. Magnetic materials and non-magnetic are separated using an applied magnetic field. The MNPs are effective adsorbent owed to their large specific surface area in addition to magnetic properties to allow the effective separation in the short time using an external magnetic field. However, the nano sized Fe$_3$O$_4$ MNPs suffer from some shortcomings such as low chemical stability, agglomeration which makes its industrial applications inconvenient [5–7]. Therefore, fabrication

of nanocomposites is a subject of great importance in developing functional nanomaterials such as catalysts [8], nano medicines [9], electronic materials [10], and pollutant scavenger [11]. Various kinds of nanomaterial components, such as 0-dimensional particles [12], 1-dimensional tubes [13] or fibers [14] and 2-dimensional nanosheets [15], have been utilized to fabricate nanocomposites having various functionalities. Especially, 2-dimensional nanosheets have attracted interests to prepare nano composites for catalysts [16], electrodes [17], and energy storage [18], due to their high specific surface area, unusual physicochemical property resulting from anisotropic structure and controllable compositions. Among the 2-dimensional nanosheets, layer double hydroxide has proven to be the suitable and easily accessible materials to stabilize the MNPs [19–24].

The shape and characteristics of layered double hydroxides were first demonstrated by powder XRD by Allmann and Taylor [25, 26]. Layered double hydroxides (LDHs) with the common formula [M$_{1-x}^{2+}$M$_x^{3+}$ (OH)$_2$]$^{x+}$ (A^{n-})$_{x/n}$· m H$_2$O, where M^{2+} and M^{3+} are divalent (e.g. Mg^{2+}, Co^{2+}, Ni^{2+}, Cu^{2+}, Zn^{2+}) and trivalent cations Fe^{3+}, Al^{3+}, Ga^{3+}), respectively; x, ranging from 0.20 to 0.33, stands for molar fraction of M^{3+} in the meatalic ions; and A^{n-} can be almost

✉ Cheera Prasad
    prasadsep20@gmail.com

    Hua Tang
    huatang79@163.com

1   School of Materials Science and Engineering,
    Jiangsu University, Zhenjiang 212013, Jiangsu,
    People's Republic of China

any organic or inorganic anion. Furthermore, the ascendancy of employed LDHs as a adsorbent of powerful photo catalysts with collective active sites are based on the following characteristics: (i) the layered structures are collected of enormously hydroxylated surfaces which were earlier described to increase the photo catalytic activity [27, 28], (ii) the flexibility of the brucite-like sheets composition which may permit the insertion of strategic cations, such as Co^{2+} and Al^{3+} within the LDHs network and, therefore, might act as charge separation centers enhancing the competence in subsequent applications [29], (iii) brucite type layers can be supplied a good metal dispersion within the layers.

Consequently, the combination of Fe_3O_4 MNPs and LDHs were evolved recently to improve separation and reproduction of the catalyst from water. The novel magnetic Fe_3O_4/LDHs nano composites can be used in a variety of applications, with targeted drug delivery [30], magnetic resonance imaging [31], photo catalysis [32, 33] and environmental remediation [34–37]. Overall, an optimal magnetic Fe_3O_4/LDHs photocatalytic structure aims to meet the following requirements. (i) The synthesis and the manufacturing process are both simple and easy with high-yield. (ii) Magnetic Fe_3O_4/LDHs composite system displays superior photocatalytic performance remarkably better to existing naked Fe_3O_4 and pure layered double hydroxides sample. (iii) Magnetic Fe_3O_4/LDHs photocatalyst must be recycled through an external magnetic field that make easy regeneration and reuse. Eventually, the Fe_3O_4/LDHs photocatalyst must have a good photo corrosion resistance ability and must be stable at room temperature few days. Some review articles are available on individual LDHs and magnetic iron nanoparticle that focus on the preparation and their catalytic applications [38–43]. Daud et al. was studied graphene/layered double hydroxides nanocomposites evaluated the research progress and new developments in the area [44]. Herein, the techniques employed for the preparation of magnetic Fe_3O_4/LDHs nanocomposites and their novel potential applications in the area of photo catalysis and environmental remediation. The best of our knowledge, this is the first review with the most recent growth in the field of magnetic Fe_3O_4/LDHs nanocomposites.

Properties of magnetic Fe_3O_4 nanomaterials, LDHs and Fe_3O_4/LDHs nanocomposite

## Properties of magnetic Fe_3O_4 nanomaterials

Over 60 years Fe_3O_4 MNPs have been adapted in the application in vitro diagnostics [45]. Over the past few decades, the Fe_3O_4 MNPs were found in a variety of structures and morphologies because of the importance of fundamental research. Conversely, the nontoxic and stable magnetic iron

oxide nanoparticles were applied in various fields such as separation and detection of proteins [46], immunoassay [47], to improve the sensitivity of magnetic resonance imaging [48], drug and gene delivery [49–51], etc. However, the use of the Fe_3O_4 MNPs has also a lot of concentration in the field of catalysis [52], bio-sensing applications [53], targeted drug delivery [54, 55], cancer therapy [56], proton exchange membrane [57], sensor [58], and magnetic resonance imaging [59, 60]. Choi and co-workers Fe_3O_4 nanoparticles are made of different shapes including solid nanospheres. Every magnetite nanoparticle showed ferromagnetic behavior with different values of coercivity (Hc) and saturation magnetization (Ms) and these values are highly depended on the shape owing to their shape, spin disorder, surface anisotropy and grain size [61]. As shown in Fig. 1a coercivity (HC), remanence magnetization (Mr), the saturation magnetization (MS) can be obtained from the hysteresis loops. The backward and forward magnetization curves overlap completely [62, 63]. Many synthetic techniques have been developed to prepare magnetic Fe_3O_4 MNPs such as sol–gel [64], hydro thermal/solvothermal [65], sonochemical [66], micro-emulsion [67] and co-precipitation methods [68, 69]. Except for the above methods, other chemical or physical methods can also be employed to synthesize magnetic iron oxide nanoparticles, such as the electrochemical methods [70–72] flow injection synthesis [73] aerosol/vapor methods [74–76], etc.

Properties of LDHs

Layered double hydroxides (LDHs) and host–guest complexes are two of the most techno logically promising inorganic systems, because of the mesoscopic controllability of their crystallite size and size distribution, the microscopic controllability of nature and amount of interlayer anions and the microscopic controllability of their layer chemical composition [77–80]. Layered double hydroxides (LDHs) are a group of anion-intercalated inorganic functional materials, which are also known as hydrotalcite-like compounds or anionic clays due to some of their interesting properties, such as high chemical and thermal stability, intercalated anions with interlayer spaces, ease of synthesis, unique structure, uniform distribution of different metal cations in the brucite layer, surface hydroxyl groups, flexible tunability, oxobridged linkage, swelling properties and ability to intercalate different type of anions [81, 82]. The lamellar structure of LDHs is based on positively charged brucite-like sheets with anions and water molecules intercalated between the layers (Fig. 1b) [83]. The specific surface area of LDHs is 20 to 120 m^2/g [84]. After calcination, LDHs can be changed into layered double oxides (LDOs) with spines or mixed metal oxides as the main component. An important property of LDO is the "memory effect" which means that this calcined product can reconstruct LDHs original layered structure via

Fig. 1 **a** Schematic presentation of the, typical hysteresis loops of magnetic iron oxide nanoparticles, **b** the structure of LDHs, **c** the synthesis of novel Fe_3O_4/MgAl–LDH porous microspheres (the figures are adopted and reproduced with permission from Refs. [83, 95, 136])
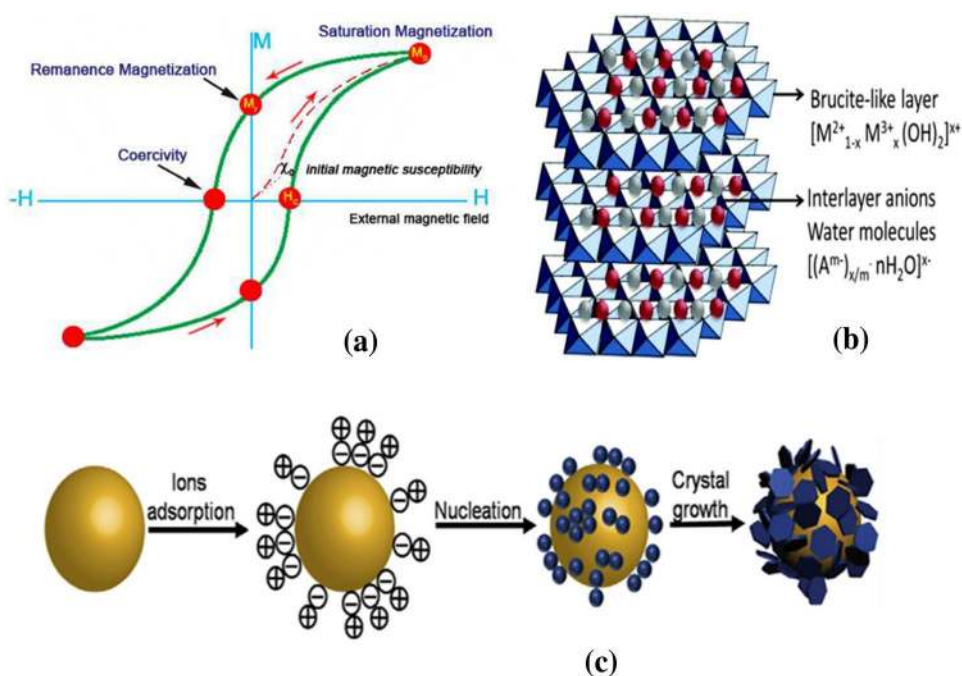
rehydration and simultaneous incorporation of anions into the interlayer from aqueous solution. LDOs that work as good catalyst for various chemical reactions of metal cations and high surface area [85]. LDHs also extensively catalyzed by strong interactions between LDHs and the arranged metals [86]. In addition, LDHs have very attractive properties, such as anion exchangeability, biocompatibility and composition flexibility [78, 87].

Properties of Fe_3O_4/LDHs nanocomposite

The preparation of Fe_3O_4 MNPs and layered double hydroxides nanocrystals by electrostatic interaction between the two samples. Magnetic Fe_3O_4 MNPs and LDHs have negatively and positively charged surfaces, respectively. In addition, as nanomaterials, both LDHs and Fe_3O_4 MNPs meet the general problem of aggregation during their application. But, Fe_3O_4/LDH nano composites, the drawback of aggregation is successfully restricted. Their self-assembly, Fe_3O_4 and LDHs can be simply got by a direct mixing method. As a result the nanocomposite sample produces constant suspension in the aqueous solution and is instantly separated to an external magnetic field. Nano hybrids species developed include new class of magnetic Fe_3O_4/LDH nano composites that may hold great potential for photo catalysis and environmental remediation. Basically, the removal of LDHs sorbents form aqueous solution was every time hard because it has a platelet-like shape which tends to diffuse in aqueous solution. Successfully hybrid of magnetic particles with LDHs were prepared and examined for various applications such as degradation of dyes [88], protein separation

[89], humic acid [90], phosphate removal [91] and drug delivery [92]. In Fig. 1c, it hesitantly proposes a formation mechanism of the present magnetic Fe_3O_4/MgAl-LDHs, which is relatively special from the reported LDHs vertically and horizontally oriented nanohybrids Fe_3O_4/MgAl-LDHs [93–95]. Furthermore, the SEM, TEM and EDX analyses confirmed that the magnetic nanocomposite of LDHs and Fe_3O_4 was synthesized and stable in aqueous solution via electronic interaction forces [96]. The electronic interaction between the negatively charged magnetite nanoparticles and positively charged LDHs was sufficient to induce stable self-assembly of the two components. This interaction can form a stable colloidal suspension of the composite in aqueous solution [88].

Synthesis of magnetic Fe_3O_4/LDHs nanocomposites

Many methods were employed to synthesize magnetic Fe_3O_4/LDHs nanocomposites. Co-precipitation is a well-known technique which is frequently used. Another well-known synthesis method is the hydrothermal method. Moreover, solvothermal reaction and exfoliation-reassembly methods are also used to synthesize magnetic Fe_3O_4/LDHs nanocomposites. The use of various preparation methods may control the shape and structure of the magnetic Fe_3O_4/LDHs nanocomposites, thus influencing its catalysis ability. To provide a complete understanding of magnetic Fe_3O_4/LDHs nanocomposites, in this part, we briefly were

given the preparation methods of magnetic Fe_3O_4/LDHs nanocomposites.

Co-precipitation synthesis

Co-precipitation Fe_3O_4/LDHs nanocomposites provide the conventional approach to the synthesis of nanohybrid. However, co-precipitation can generate wide particles size distributions with an average size ranging from submicron to tens of microns if the essential safety is not taken. Sometimes calcined powder sometimes needs to be strapped to contribute to the reduced purity to achieve the desired particle size. In the case of LDHs as photocatalyst co-precipitation is the mostly used technique accepted by researchers. Garcia et al. reported a common co-precipitation method for the synthesizing of Zn–Cr LDHs with NaOH and urea solution as precipitators for photocatalytic applications [97]. The co-precipitation technique is a method that is employed widely for the preparation of a different of LDHs and novel magnetic Fe_3O_4 nanoparticles-based composites such as Fe_3O_4/LDHs [95, 98]. The illustration of the formation of Fe_3O_4/LDHs hybrid is shown in Fig. 2a. Initially, megnisium and aluminium nitrates with a Mg/Al molar ratio of 2:1 have been added in 100 mL of water. The pH of the solution has been modified using the mixture of 0.02 M $NaNO_3$ and 2 M NaOH with constant stirring for 2 h. Consequently, about 20 mL of Fe_3O_4 sample added with the above solution. The prepared samples are referred here as Fe_3O_4/Mg_2Al–NO3–LDHs [99, 100]. One of the common differences in the use of this method is to use a variety of pH to precipitate hydroxides. The other distinction includes different concentrations of the precursor that can vary from diluting to concentrated solutions. The two factors, concentrations and pH, perhaps the effects are actually not literary but may influence the features. For example, Fe_3O_4/Mg–Al–CO_3–LDHs has been explored by Ran-ran Shan, [101] at pH 9–10. Fe_3O_4/CuMgAl-LDHs was investigated by Zhang et al. [102] at pH 10. Core–shell Fe_3O_4/Mg_3Al–CO_3–LDHs were explored by Yan et al. [103] at pH 10. The synthesis of magnetic Fe_3O_4/LDHs nanocomposites using various methods and application shown in Table 1.

Hydrothermal syntheses

Hydrothermal method is a typically important technique to synthesize Fe_3O_4/LDHs nano composites. Hydrothermal synthesis is a solution reaction based approach. In a broader sense, it can be defined as the method for making materials from room temperature to high-temperature solutions. To control the morphology of the materials to be prepared, either low pressure or high-pressure conditions may be used depending on the vapor pressure of the main composition in the reaction. This is very easy and credible method for the preparation of Fe_3O_4/LDHs nanocomposites through hydrothermal process which high purity Fe_3O_4/LDHs nanocomposites may be obtained. Herein, the solution obtained through co-precipitation method after the sample stirring is transferred to a Teflon-lined autoclave at certain temperature and time for the pressure maintained in the autoclave allows the boiling point of the

Fig. 2 **a** The co-precipitation synthetic strategy of Fe_3O_4@Mg_3Al–CO_3 LDHs, **b** hydrothermal synthetic strategy of Fe_3O_4/LDHs nanocomposites (the figures are adopted and reproduced with permission from Ref. [103, 104])
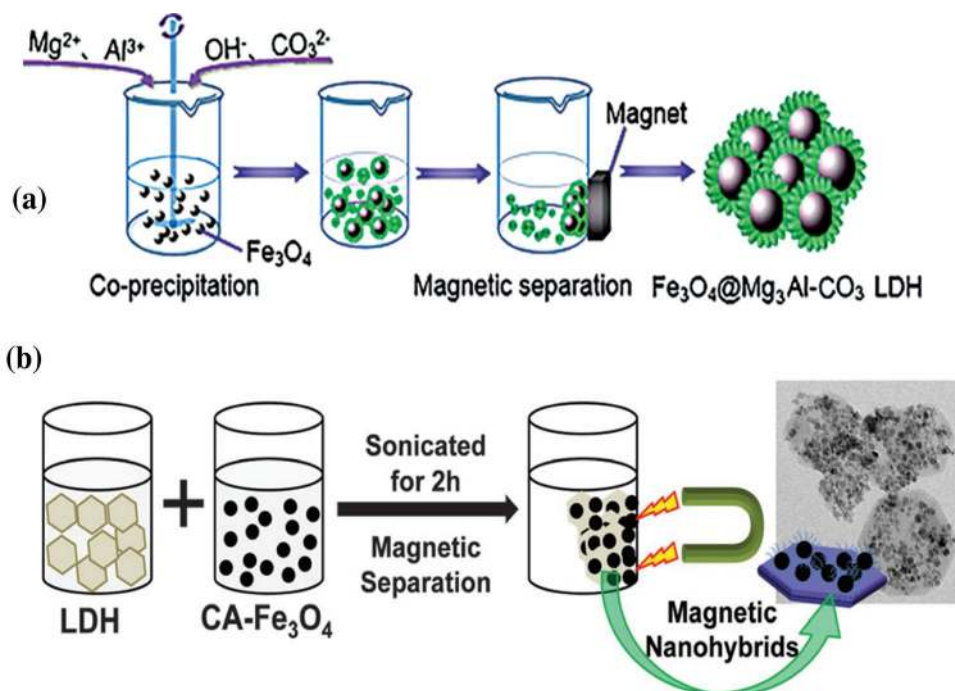
Table 1 Synthesis and applications of magnetic Fe_3O_4/LDHs nanocomposites

Nanocomposite	Synthesized method	Size	Applications	References
Fe_3O_4/MgAl–LDH	Co-precipitation synthesis	40–100 nm	Adsorption properties of dye from water	[95]
(Mg/Al + Fe)-CO_3 LDHs	Co-precipitation synthesis	–	Photo catalytic activity for H_2 generation	[98]
Fe_3O_4/MgAl-LDHs	Co-precipitation synthesis	–	Adsorption of Cd(II)	[101]
Core shell Fe_3O_4/CuMgAl-LDHs	Co-precipitation synthesis	100–200 nm	Hydroxylation of phenol	[102]
Core–shell Fe_3O_4/Mg_3Al–CO_3 LDH	Co-precipitation synthesis	300–350 nm	Anionic dye removal from wastewater	[103]
LDHs/Fe_3O_4 magnetic nano hybrids	Mixed method (co-precipitation synthesis and hydrothermal method)	240 nm	Thermo-chemotherapy	[104]
Mg/Al LDHs/Fe_3O_4 nano composites	Two-step wet chemistry route	10–20 nm	Removal of humic acid	[90]
Fe_3O_4/(Cu/Ni)–Al LDHs	Co-precipitation synthesis	10 nm	Degradation of methylene blue	[96]
Fe_3O_4/sulfonated β-cyclodextrin intercalated LDHs	Co-precipitation method	200 nm	Methylene blue removal	[137]
Fe_3O_4@C@Ni–Al LDHs	Two-step layer-by-layer route	10 nm	Separation of uranium	[120]
Fe_3O_4/ZnCr LDHs	Two-step microwave hydrothermal method	10 nm	Organic dyes wastewater treatment	[105]
Fe^{3+}doped Mg/Al/LDHs	Solvothermal method	35–70 nm	UV lights hielding coatings	[107]
Fe_3O_4/ZnAl–LDHs	Co-precipitation method	–	Removal of Cr(VI)	[123]
Fe_3O_4@DFUR–LDH	Co-precipitation	10–20 nm	Magnetically controlled drug delivery	[94]
NiAl-LDH/Fe_3O_4-RGONanocomposites	Hydrothermal route	15 nm	Degrade ciprofloxacin (CIP)	[106]
Fe_3O_4/Mg_2Al-NO_3-LDHs	Co-precipitation method	–	Remediation of aqueous phosphate	[100]
Fe_3O_4@MgAl–LDH@Ce_3W_{18} nano composite	Selective ion-exchange method	10–40 nm	Degradation of methylene blue	[138]
Fe_3O_4@MgAl–LDH@Au	Solvothermal method	100–200 nm	Catalytic oxidation of alcohols	[93]
Fe_3O_4/ZnCr LDHs	Two-step microwave hydrothermal method	20 nm	Efficient removal of dyes and heavy metal wastewater	[139]
Fe_3O_4/MgAl-LDH composite	Co-precipitation method	–	Three red dyes (reactive red (RR), congo red (CR) and acid red)	[140]
Fe_3O_4@CuNiAl-LDH	Co-precipitation method	100 nm	–	[141]
magnetite-graphene (MG) and Mg/Al LDHs	Hydrothermal process	1436.8 nm	Adsorption of arsenate	[119]
Fe_3O_4/MTX-LDH/Au nanoparticles	Co-precipitation	255–270 nm	For cancer therapy	[135]
Fe_3O_4/SiO_2/NiAl-LDH microspheres	Situ growth method	300 nm	Magnetic separation of proteins	[142]
Fe_3O_4/GO/LDHs composites	Mechano hydrothermal route	200 nm	For removing the heavy metal Pb(II) and the hydrophobic organic pesticide 2,4-dichlorophenoxyacetic acid	[19]

aqueous solution to increase, thereby preventing evaporation and allowing nucleation to occur. Optimization of the sizes and structures of the Fe_3O_4/LDHs nanocomposites may be achieved through changes in the experimental parameters such as mixing time, pH, heating duration and heating temperature. In this method, Prasadarao et al. has been investigated Fe_3O_4/ZnCr LDHs composites for study the themo-chemotherapy [104]. An illustration of this method is presented in Fig. 2b. Another study also addressed synthesis of Fe_3O_4/LDHs nanocomposite. Dan Chen and his co-workers have successfully synthesized the magnetic Fe_3O_4/ZnCr LDHs composites for the removal of heavy metal ions and organic dyes degradation [105].

The hydrothermal synthesis is more advantage than co-precipitation method due to the well crystallized sample with uniform morphology [106].

Solvothermal reaction

Solvothermal route is one of the most frequent and efficient preparation methods to make the Fe_3O_4/LDHs nanocomposites with different of morphologies. In this method, the autoclave is filled with water or organic compounds to take reaction in high temperature and pressure conditions [107]. If the nonaqueous solution is used as medium reaction, it is called a solvothermal method. This route can help and speed

up the reaction among the reactants, promote hydrolysis, followed by crystal growth resulting in self-assembly of Fe_3O_4/LDHs nano composites in the solution. Furthermore, the characteristics, morphology, size and structures of Fe_3O_4/LDHs nanocomposites can be adapted easily by varying the different reaction parameters, such as reaction medium, reaction time, pressure, pH and concentration of the reactants and filled volume of autoclave. This method can be suitable for the preparation of Fe_3O_4/LDHs nano composites with a variety of shapes as compared to other methodologies. For example, 0.104 g Fe_3O_4 nanoparticles have been dissolved into a 100 mL nonaqueous solution under ultra sonication. To maintain the pH (10), they have been added the mixture of alkaline solution containing Na_2CO_3 and NaOH. Furthermore, another 100 mL nonsolution containing 2.310 g $Mg(NO_3)_2 \cdot 6H_2O$ and 1.125 g $Al(NO_3)_3 \cdot 9H_2O$ has been mixed drop wise into the above suspension. The obtained sample has been kept at 60 °C for 24 h. The prepared sample was separated using a magnet, washed by deionized water for five times and then dried at 60 °C for 24 h giving the product Fe_3O_4/MgAl-LDHs [93].

Applications

At present, most scientific attraction of magnetic Fe_3O_4/LDHs nanocomposites. These composites have been explored for their applications in environmental remediation and photo catalysis. This segment focuses on the concert of different magnetic Fe_3O_4/LDHs nano composites used in different applications. Moreover, adsorption of containments in wastewater equivalent to air pollution, water pollution is another world wide environmental anxiety. The effective approaches of water purification can be categorized into pollutants conversion and adsorption. For the pollutants mainly organic dyes and heavy metal ions in wastewater that strongly threaten animals, human and plants, magnetic Fe_3O_4/LDHs nanocomposites typically show strong binding with these pollutant species.

Photoreduction of organic dyes

Photocatalytic degradation has given an aqueous solution to organic pollutants by completely changing molecular to mineral acids, H_2O and CO_2 [108, 109]. Nevertheless, taking into account economic cost and the large band gap they are inappropriate for amazing huge amounts of wastewater. The hybrid of Fe_3O_4 MNPs and LDHs nanocomposite is favorable approach for environmental remediation. A few
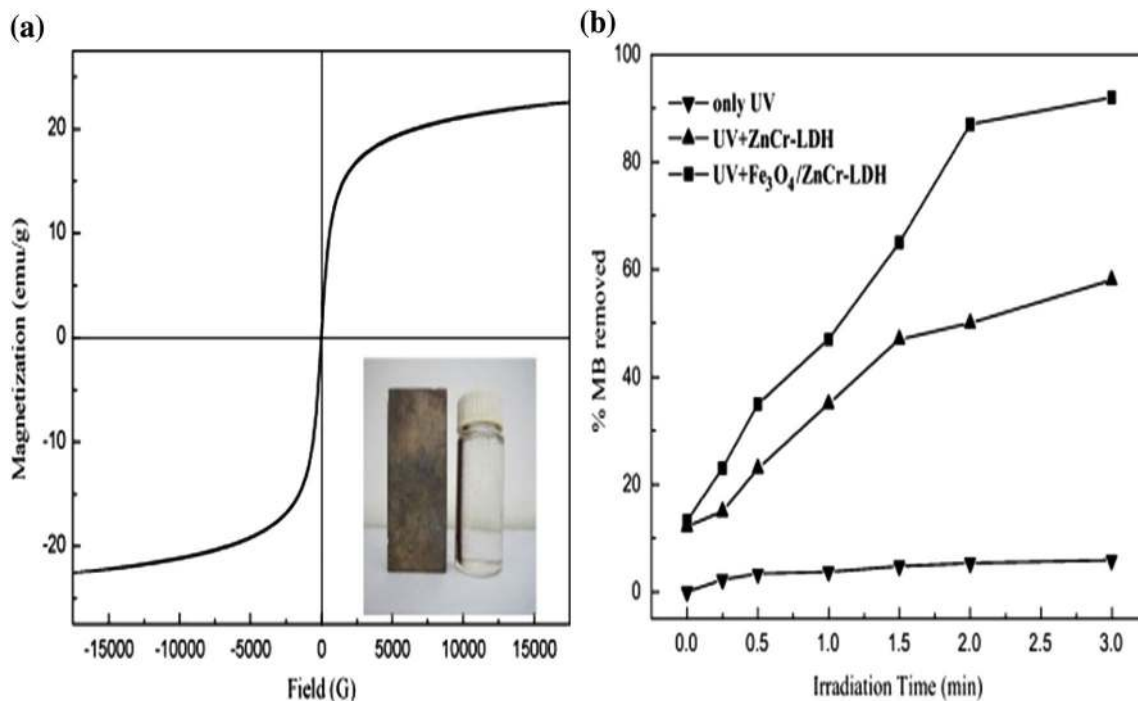

Fig. 3 **a** Magnetization characteristic curve of Fe_3O_4/ZnCr-LDH, the inset of figure is the photographs of the magnetic composite in aqueous solution. **b** The photodegradation of MB by Fe_3O_4/ZnCr-LDH and ZnCr-LDH photocatalysts as a function of UV light irradiation time (the figures are adopted and reproduced with permission from Ref. [105])

published studies are available for the preparation of Fe_3O_4/LDHs nanocomposites and their photocatalysis application. Chen et al. photocatalytic Fe_3O_4/ZnCr LDHs composites was effectively explored through the two step micro hydrothermal technique [105]. The magnetic separation of such a Fe_3O_4/LDHs material has been investigated in aqueous solution by putting the magnet near the glass, evidently showing the magnetic characteristics of materials Fig. 3a. For that reason, separating the magnetic Fe_3O_4/ZnCr LDHs nanohybrids quickly changes in the environmental remediation. Methylene blue (MB) is widely used for photocatalytic studies as a model dye. The MB stability increases against photo catalysis when the pH reduced, but the amendment of the pH to lower values than 5.4 will lead to the dissolution of hydrotalcite [110]. After 3 h at room temperatures in the presence of Fe_3O_4/ZnCr LDHs nanocomposite could remove ~95% of total MB in aqueous solutions Fig. 3b. This is much being better than the ZnCr LDHs samples (degrade only 58.1% under UV-light in 3 h.) due to Fe_3O_4/ZnCr LDHs nanocomposites demonstrated essentially higher catalytic activity, this could be attributed to the effect of the increased surface area and the unique advantage of easy separation under external magnetic fields. These results proved that the

modification of Fe_3O_4 nanoparticles on the LDHs surface added to the superior photocatalytic power of ZnCr LDHs.

Hamid et al. reported that the Cu/Ni–Al LDHs/Fe_3O_4 nanocomposite has been synthesized by co-precipitation method [96]. As shown in Fig. 4a, magnetic Fe_3O_4 as a core was synthesized by co-precipitation of Fe^{2+} and Fe^{3+} in aqueous solution. The nanocomposite was then prepared by coprecipitation of Cu^{2+}, Ni^{2+}, and Al^{3+} metal ions on the Fe_3O_4 core nanoparticles in the alkaline medium. The composition of the (Cu/Ni)–Al LDHs/Fe_3O_4 composite was investigated by EDX (Fig. 4b). Clearly, Ni, Cu, Al, and O elements were all present in the (Cu/Ni)–Al LDHs/Fe_3O_4 composite. However, the (Cu/Ni)–Al LDHs/Fe_3O_4 composite contained all of these elements as well as Fe, providing the best evidence for the formation of the magnetic nanocomposite. The results of these analyses, therefore, confirm that the magnetic nanocomposite of LDHs and Fe_3O_4 was synthesized and stable in aqueous solution via electronic interaction forces. The electronic interaction between the negatively charged magnetite nanoparticles and positively charged LDHs was sufficient to induce stable self-assembly of the two components. This interaction can form a stable colloidal suspension of the composite in aqueous solution.
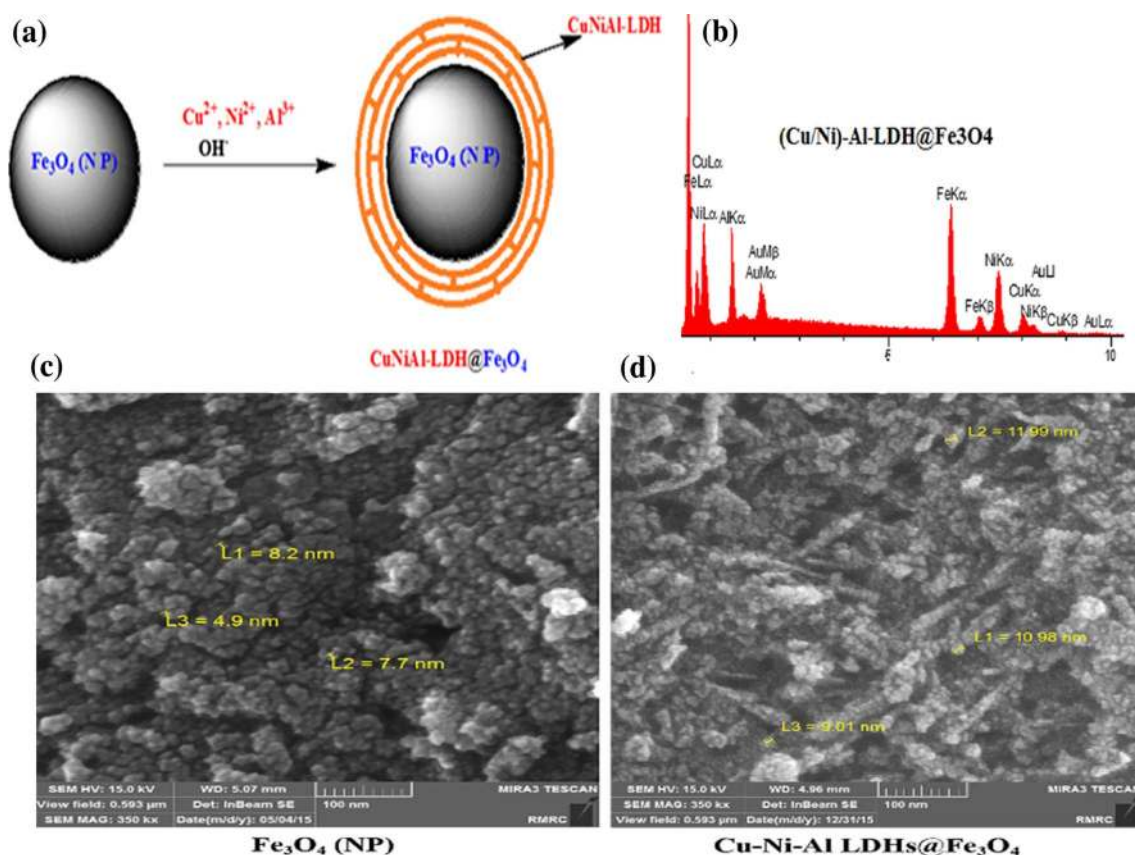

Fig. 4 **a** Synthesis route for (Cu/Ni)–Al LDHs/Fe_3O_4 magnetic nanocomposite. **b** EDX data of (Cu/Ni)–Al LDHs/Fe_3O_4 nanoparticles. **c, d** SEM images of Fe_3O_4 and (Cu/Ni)–Al LDHs/Fe_3O_4 powder (the figures are adopted and reproduced with permission from Ref. [96])

Furthermore, SEM images of Fe_3O_4 and (Cu/Ni)–Al LDHs/ Fe_3O_4 are shown in Fig. 4c, d. The morphology of all the compounds was sub-micro-spheres with diameter of about 4–10 nm, but the surface of the (Cu/Ni)–Al LDHs/Fe_3O_4 nanocomposite showed rougher sheet-like morphology than the surface of Fe_3O_4. Photodegradation of Methylene blue as an organic pollutant by this nanocomposite via oxidation under visible-light irradiation has been studied in comparison with Fe_3O_4 and (Cu/Ni)–Al LDHs. The results demonstrated that the degradation by the nanocomposite was more efficient compared with Fe_3O_4 or (Cu/Ni)–Al LDHs alone. After four runs of use as photo catalyst, the composite remained powerful and effective in the degradation reaction.

Ni and coworkers also decorated NiAl-LDHs and Fe_3O_4 NPs on the surface of graphene oxide through a simple hydrothermal route [106]. The results demonstrated that Fe_3O_4 nanoparticles and NiAl-LDH nanoplatelets size about 15 nm were homogeneously tailored on the surface of graphene oxide. The as prepared Fe_3O_4-RGO/NiAl-LDHs nanocomposites were studied to adsorption ciprofloxacin (CIP) in water under visible light irradiation. As shown in Fig. 5a, the NiAl-LDH/Fe_3O_4-RGO composite displayed much better photocatalytic activities than that of NiAl-LDH/RGO, Fe_3O_4/RGO, NiAl-LDHs samples. They were in the order of NiAl-LDH/Fe_3O_4-RGO > NiAl-LDH/ RGO, > Fe_3O_4/RGO > NiAl-LDHs. However, as depicted in Fig. 5b, the reaction rates of NiAl-LDH/Fe_3O_4/RGO, NiAl-LDH/RGO, Fe_3O_4/RGO and NiAl-LDHs to be 0.235 min^{-1}, 0.01579 min^{-1}, 0.00183 min^{-1} and 0.0087 min^{-1},

respectively. It revealed superior photo catalytic activity compared to pure NiAl-LDHs which degradation rate of the synthesized NiAl-LDH/Fe_3O_4-RGO was 1.5 and even 3 times faster than that of NiAl-LDH/RGO and pure NiAl-LDHs, respectively. The electron transfer and photocatalytic mechanism of NiAl-LDHs/Fe_3O_4-RGO are schematically demonstrated in Fig. 5c. Electrons (e^-) in the valence band (VB) of NiAl-LDHs are rapidly elevated to the conduction band (CB) with concurrent formation of holes (h^+) in the valence band once irradiate by visible light. The work function of graphene, Fe_3O_4 and the conduction band (CB) of NiAl-LDHs are 4.42, 1.0 and − 1.1 eV, respectively. Owed to the CB of NiAl-LDHs is smaller than the work function of graphene, the photo generated electrons in the CB of NiAl-LDHs would competently migrate into the unoccupied electron level of graphene sheets, which are very well and successfully decorated by NiAl-LDHs nanoplatelets. Moreover, the NiAl-LDH/Fe_3O_4-RGO nanocomposites exhibited magnetically separable ability and stable catalytic activity, which is beneficial to its practical application. The pollutants would not only be adsorbed on the surface of Fe_3O_4/ LDHs, but also be degraded, and this can greatly increase the wastewater treatment capacity.

Magnetic Fe_3O_4/LDHs nanocomposites for organic dyes adsorption

The organic dyes are widely utilized in industries including food, cosmetics, leather and textile. Nevertheless, various

Fig. 5 a Photodegradation of CIP as a function of absorption and irradiation time over different photocatalysts: without catalyst, NiAl-LDHs, Fe_3O_4/ RGO, NiAl-LDHs/RGO, and NiAl-LDHs/Fe_3O_4/RGO. **b** The pseudo-first-order dynamic curve of ln (C_0/C) with time for the photodegradation of CIP over different photocatalysts: without catalyst, NiAl-LDHs, Fe_3O_4/RGO, NiAl-LDHs/RGO, and NiAl-LDHs/Fe_3O_4/RGO. **c** The schematic illustration of photocatalytic reaction mechanism over NiAl-LDHs/Fe_3O_4– RGO composite (the figures are adopted and reproduced with permission from Ref. [106])
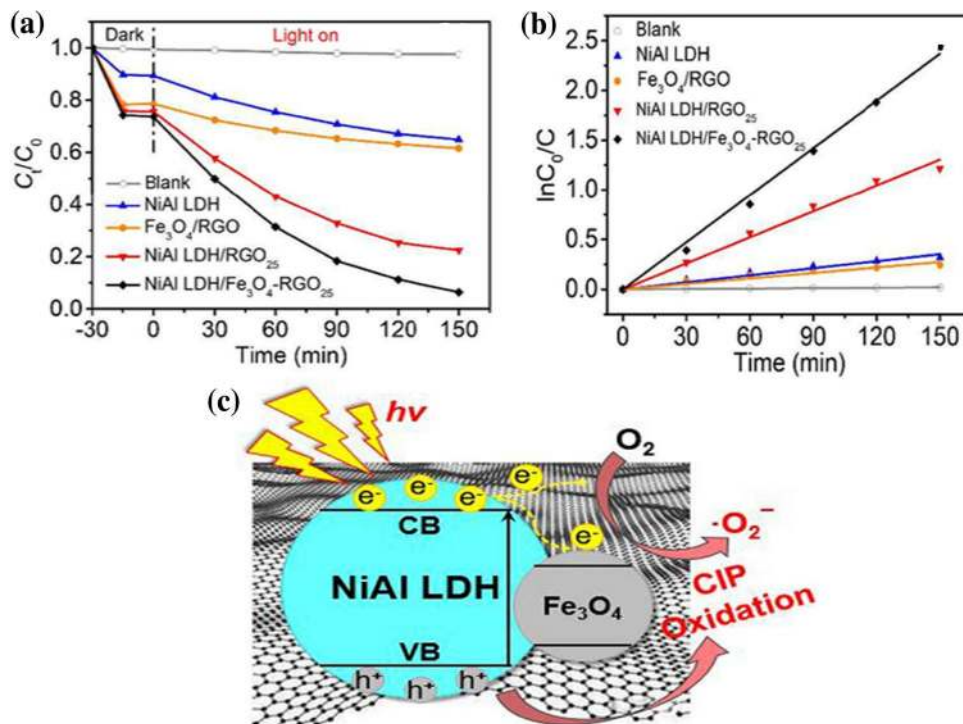
dyes are toxic to microorganisms and harmful to human being, therefore, the exclusion of dyes has been increased more attention over the past few years [111]. A variety of chemical and physical methods such as coagulating sedimentation [112], adsorption [113] chemical oxidation, were studied to degrade the organic dyes from contaminating water. Among these methods, adsorption is extensively utilized techniques for the degrade of organic dyes in a water solution [114–116].

Lu et al. has been explored the spectral and organic dyes degradations by integrating magnetic Fe_3O_4 nanoparticles with layered double hydroxides via co-precipitation synthesis [95]. The synthesized Fe_3O_4/MgAl-LDHs nanocomoposite exhibits a novel morphology with LDHs to the surfaces of Fe_3O_4 nanoparticles. The prepared Fe_3O_4/MgAl-LDHs nanocomposites show excellent degradation efficiency for eliminating the Congo red dye from aqueous solution. The shape and structure of synthesized nanocomposite were determined by TEM analysis. Figure 6a shows the TEM images of the Fe_3O_4/MgAl-LDHs nanocomoposite, which obviously represents core shell structure. The resulting sample average particles size is in the range of 40–100 nm. Commonly, the magnetic property of the resulting sample is dependent on particles size, structure and morphology which are influenced by the manufacturing process. Figure 6b shows the magnetic hysteresis loops of the Fe_3O_4/MgAl-LDHs and Fe_3O_4 nanoparticles. The experiential saturation magnetization (M_s) of both Fe_3O_4/MgAl-LDHs and Fe_3O_4 nanoparticles are 38 and 79 emu/g. The schematic diagram of adsorption mechanism of Fe_3O_4/MgAl-LDHs were proposed and showed in Fig. 6c. Adsorption takes place at the surface of Fe_3O_4/MgAl-LDHs magnetic microspheres

through electrostatic forces of attraction for CR, pursued by intercalation of CO_3^{2-} anion, which were consequently changed by SO_3^- anion of CR via anion exchange.

To extend the research on magnetic Fe_3O_4/MgAl-LDHs nanocomposite, Moaser et al. synthesized cauliflower-like Fe_3O_4/MgAl-LDH/Ce_3W_{18} nanocomposite through the selective ion-exchange technique [93]. The as prepared Fe_3O_4 nanoparticles were spherical shape with an average size of 130 nm. Moreover, Fe_3O_4 nanoparticles were homogeneously dispersed on LDHs. The vibrating sample magneto meter analysis of the nanocomposite explains that the magnetic saturation (Ms) values of the Fe_3O_4/MgAl-LDH and Fe_3O_4/MgAl-LDH/Ce_3W_{18} are lower than bare Fe_3O_4 due to the non-magnetic LDHs layer coated on the magnetic Fe_3O_4 surface. The catalytic properties of Fe_3O_4/MgAl-LDH/Ce_3W_{18} have been explored by degradation reaction of Rhodamine B, Methylene Blue and Methyl Orange dyes with the help of H_2O_2 at room temperature.

Furthermore, various authors conducted similar studies to examine the absorbance of Fe_3O_4/LDHs nanocomposites and visible light activity. Chen et al. found that the efficient and easy technique for the preparation of colloidal nanocomposites containing of Fe_3O_4/MgAl-LDHs nanocrystals [88]. The TEM images of LDHs and LDHs/Fe_3O_4 NPs shown in Fig. 7. As it can be observed from Fig. 7a, LDHs consists of well-dispersed LDH nanocrystals with their sizes in a range of 50–80 nm. The image of the sample LDHs/Fe_3O_4 NPs (1:0.3) (Fig. 7b) shows that the surface of LDH nanocrystals is decorated with Fe_3O_4 NPs (in darker colors). The sizes of the Fe_3O_4 nanoparticles based on the TEM analysis are around 10 nm. The positively charged LDH nanocrystals acted as an attractive substrate for the attachment of the

Fig. 6 TEM images of Fe_3O_4/MgAl-LDHs (**a**), Magnetization curves of Fe_3O_4 and Fe_3O_4/MgAl-LDHs (**b**) and adsorption mechanism of Fe_3O_4/MgAl–LDHs (**c**) (the figures are adopted and reproduced with permission from Ref. [95])
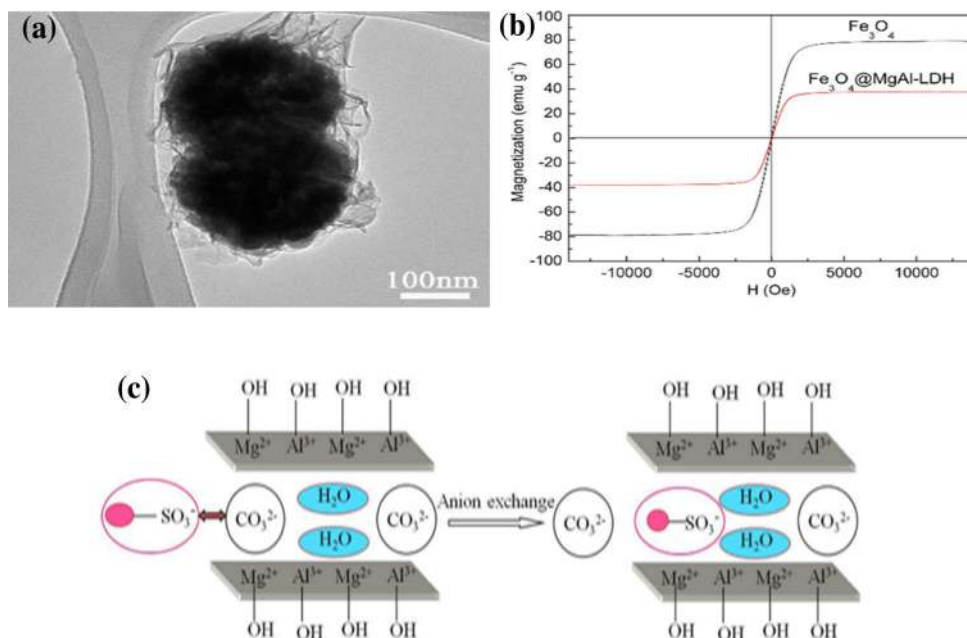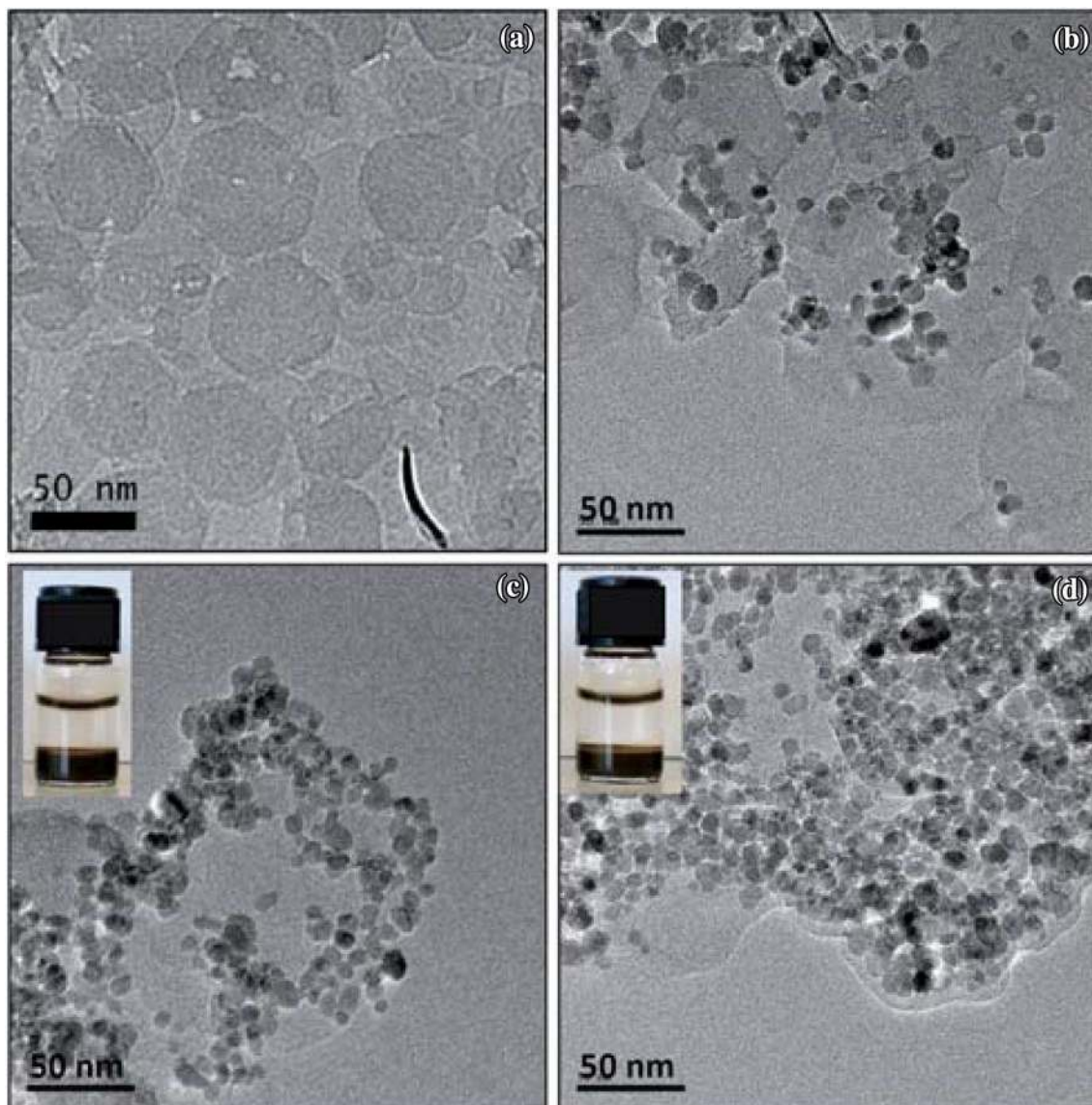
Fig. 7 TEM images of **a** LDHs, **b** LDHs/Fe$_3$O$_4$ NPs (mass ratio 1:0.3), **c** LDHs/Fe$_3$O$_4$ NPs (mass ratio 1:1), and **d** LDHs/Fe$_3$O$_4$ NPs (mass ratio 1:4). The insets in **c** and **d** show the corresponding photos of the suspensions after 24 h (the figures are adopted and reproduced with permission from Ref. [88])

negatively charged Fe$_3$O$_4$ NPs by electrostatic interaction. When the nanohybrid samples were prepared with higher proportions of Fe$_3$O$_4$ NPs (the ratio of LDHs: Fe$_3$O$_4$ NPs at 1:1 and 1:4), all Fe$_3$O$_4$ nanoparticles remain attached to the surface of LDHs. Nevertheless, they are aggregated, and the extent of aggregation increases with the increase of the nanoparticle population, as shown in Fig. 7c, d. Correspondingly, the exposed surface area of LDHs is reduced. As a result, their suspensions were not stable and the particles quickly settled as shown by the photos of Fig. 7c, d inset. However, they have been selected Congo red dye as an organic dye in this experiment. It is notable that the whole process can be concluded within 15 min due to the oxidative regeneration processes and quick adsorption.

In addition, Wang et al. has been investigated the removal of humic acid (HA) from aqueous phase using the Fe$_3$O$_4$/LDHs nanocomposites [90]. The results demonstrated that HA removal on Fe$_3$O$_4$/LDHs is weakly dependent on ionic strength and strongly dependent on pH. The removal of humic acid onto Fe$_3$O$_4$/LDHs occurs by ion exchange with both the surface anions of the LDHs and intercalated. Moreover, the equilibrium data of HA on Fe$_3$O$_4$/LDHs fitted to the Freundlich isotherm model and the maximum adsorption capacity of humic acid onto Fe$_3$O$_4$/LDHs composite

reaches 353.82 mg/g, exhibiting superior activity for humic acid removal.

## Magnetic Fe$_3$O$_4$/LDHs nanocomposites for heavy metal ion adsorption

The Fe$_3$O$_4$/LDHs nanocomposites used for adsorption should have the maximum number of active sites, high surface area and high porosity. The magnetic Fe$_3$O$_4$/LDHs nanocomposites satisfy all the mandatory features of removal of toxic metal ions. The nanocatalyst is explored mainly for the exclusion of contaminated metal ions from aqueous solution and also from the atmosphere by adsorption [117–119]. Furthermore, Fe$_3$O$_4$/LDHs nanocomposites were efficiently studied in the adsorption of heavy metals, such as chromium, Pb^{2+}, As^{3+}, Ni^{2+}, Hg^{2+} and Cd^{2+} in aqueous treatment and radioactive uranium (VI) was utilized for the adsorption of other toxic metals ions [120].

A novel magnetic Fe$_3$O$_4$/C/LDHs composite was investigated by a two-step layer-by-layer method by Zhang et al. [120]. The saturation magnetization of Fe$_3$O$_4$/C/NiAl-LDHs and Fe$_3$O$_4$/C are 2.20 and 8.25 emu/g, respectively. The magnetic Fe$_3$O$_4$/C/NiAl-LDHs has lower magnetic saturation than that of Fe$_3$O$_4$ nanoparticles due to the non magnetic nature of C and LDHs are anchored on Fe$_3$O$_4$ nanoparticles. The Fe$_3$O$_4$/C/NiAl-LDHs nanocatalyst was studied their efficiency for the removal of U(VI). When the pH value increases up to 2–5 removal efficiency increases, whereas, adsorption efficiency decreases upon the pH 5–9. At lower pH, UO$_2^{2+}$ is the predominate species of U (VI). As the solution pH is increased, the hydrolysis products such as (UO$_2$)$_3$(OH)$^{5+}$ (UO$_2$)$_2$(OH)$_2^{2+}$, and UO$_2$OH$^+$, are formed

[121, 122]. Moreover, the effect of Fe$_3$O$_4$/C/Ni–Al LDHs dosage on the removal of U (VI) through Fe$_3$O$_4$/C/Ni–Al LDHs, where they can observed that increasing the amount of adsorbent range improved the U(VI) removal efficiency. The results show that adsorption was followed the pseudo-second-order kinetic model. The adsorption isotherm data fitted well with Freundlich model and Langmuir isotherm, adsorption capacity was found to be 174.1 ± 0.2 mg/g. The results show that the synthesized Fe$_3$O$_4$/C/Ni–Al LDHs act as efficient adsorbent sample for removal of U(VI) from aqueous solutions. As well, the Fe$_3$O$_4$/C/Ni–Al LDHs nanocatalyst simply removed from the solution through a magnet after the adsorption process.

Number of magnetic Fe$_3$O$_4$/LDHs composite has been conducted by various researchers to study the adsorption of toxic metal in aqueous media. Yan et al. was reported ZnAl LDHs and Fe$_3$O$_4$/ZnAl LDHs for capable adsorption of Cr(VI) from pollute water [123]. The removal ratio of Cr(VI) is apt to reduce with the increase of solution pH. The removal of Cr(VI) on Fe$_3$O$_4$/LDHs was explored by varying pH in the range of 3.00–12.00. The pH effect on Cr(VI) adsorption can be explained by the surface properties of the adsorbents and evaluation of the solute. At lower pH, 3–6.8, HCrO$_4^-$ is the predominate ion of Cr(VI), and at higher pH 6.8–10, only CrO$_4^{2-}$ is stable [124]. The adsorption kinetic data explained well with a pseudo second order kinetic model and equilibrium data fitted well to the both Langmuir and freundlich equation. Adsorption thermodynamic showed that the removal of hexavalent chromium was endothermic and spontaneous in nature. The Fe$_3$O$_4$/ZnAl LDHs composite has a large surface area and mesoporous properties it displays superior adsorption of toxic metals from water.

Fig. 8 **a** SEM and **b** TEM images of Fe$_3$O$_4$/GO/LDHs composite (the figures are adopted and reproduced with permission from Ref. [19])
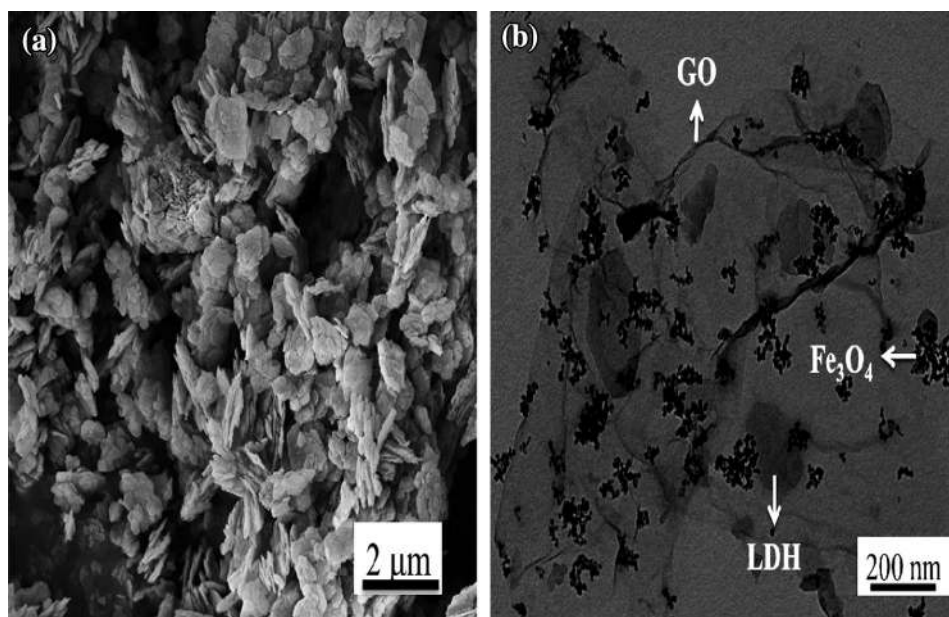
Zhang et al. has been reported magnetic Fe_3O_4/GO/LDHs composite for the adsorption of Pb(II) and 2,4-dichloro phenoxy acetic acid from water phase [19]. Figure 8 demonstrates the SEM and TEM images of the Fe_3O_4/GO/LDHs composite. The Fe_3O_4/GO/LDHs composite featured irregular flaky particles (Fig. 8a). The Fe_3O_4 sample was composed of spherical particles with a diameter of approximately 20 nm, and the GO sample was composed of wrinkled sheets each could be distinguished in the Fe_3O_4/GO/LDHs composite (Fig. 8b). As well, hexagonal crystals, typical of LDHs, were observed, and the lateral size of the LDH crystals was ~ 200 nm. In addition, both the Fe_3O_4 nanospheres and LDH crystals appeared to be anchored to the surface of GO (Fig. 8b). The BET sorption isotherms of the magnetic Fe_3O_4/GO/LDHs samples which characterize "type IV" isotherms with H3 hysteresis loops. The Fe_3O_4 and magnetic Fe_3O_4/GO/LDHs sample specific saturation magnetizations (Ms) of were 27.3 and 3.5 emu/g, respectively. The percentage removal of Pb(II) increased with an increase in pH from 2 to 5 and decreased with an increased

pH 6–9. Decrease in Pb(II) removal at higher pH is due to the formation of Pb(II) as $Pb(OH)^+$, and $Pb(OH)_2^0$ and $Pb(OH)_3^-$ at different pH values. The adsorption of Pb(II) happened mainly from the adsorption and absorption contribution of the LDHs material by surface induced precipitation of $Pb_3(CO_3)_2(OH)_2$.

Gwak et al. has been studied nanocomposites containing magnetic Fe_3O_4 nanoparticles and LDHs nanosheets were prepared by two different methods, exfoliation-reassembly and coprecipitation, for aqueous chromate adsorbent [125]. The surface morphology of exfoliation-reassembly method was smooth compared with that of co-precipitation method which showed agglomeration of small particles. Such smooth surface of nanoparticles has been reported in the nanocomposite between nanoparticles and nanosheets, suggesting house of card structure developed by reassembled nano sheets [119, 126]. Exfoliation-reassembly method and co-precipitation method showed maximum adsorption amount of 54.68 and 50.65 mg Cr(VI)/g nanocomposite after
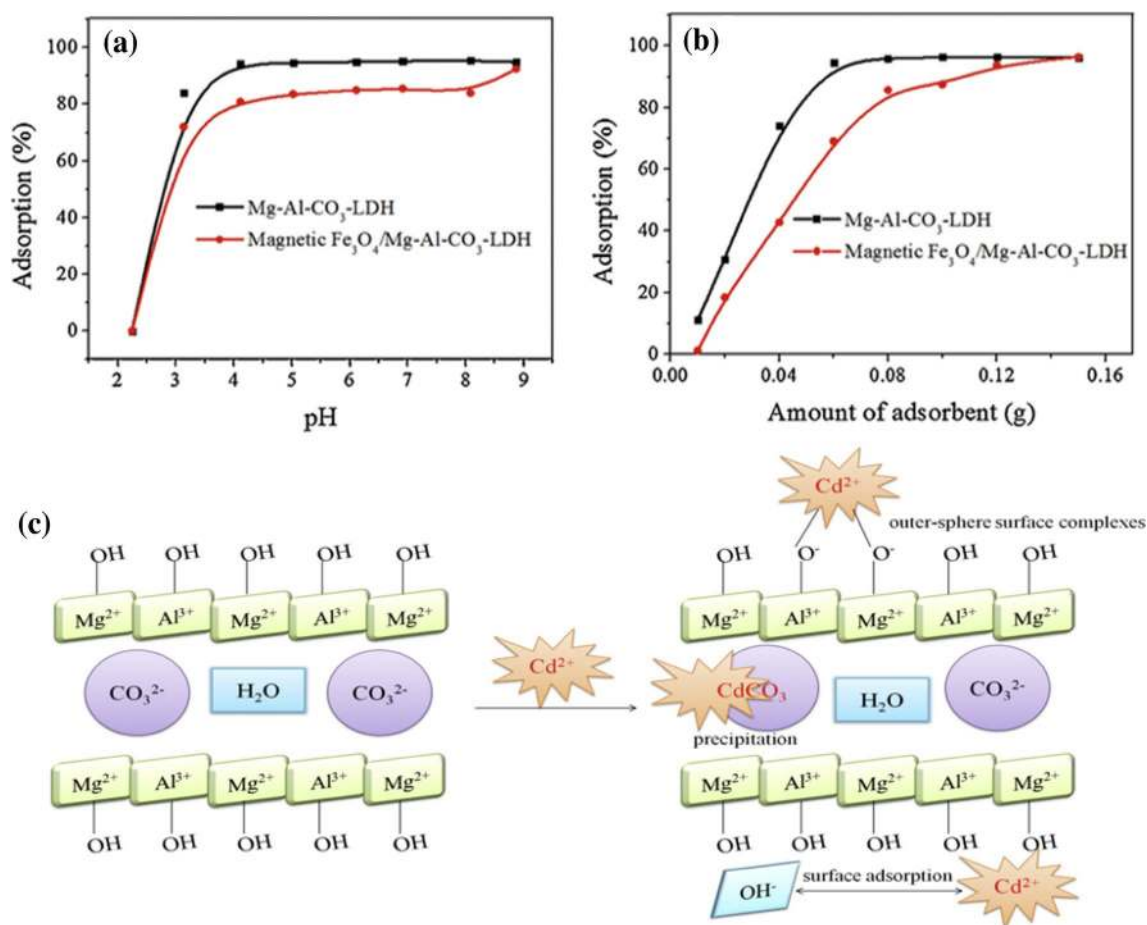

Fig. 9 a Effects of solution pH, **b** adsorbent dosage, on Cd(II) adsorption by MgAl-LDHs and magnetic Fe_3O_4/MgAl-LDHs. **c** Schematic representation of the adsorption mechanisms of Cd(II) onto MgAl-LDHs or Fe_3O_4/MgAl-LDHs (the figures are adopted and reproduced with permission from Ref. [101])

24 h, suggesting slightly enhanced adsorption efficacy of exfoliation nano composite.

Shan et al. has been reported that the removal of Cd(II) using Fe_3O_4/MgAl-LDHs composite [101]. The Cd(II) removal efficiency using Fe_3O_4/MgAl-LDHs nanocomposites increases with increasing below pH 4 followed by a decrease in efficiency as pH increases beyond 6. At low pH, removal efficiency is low because the high concentration of protons (H^+) in solution competes with the Cd(II) ions for the adsorption sites of the adsorbents. Furthermore, Cd(II) ions are prone to the formation of $Cd(OH)^+$ and $Cd(OH)_2$ Fig. 9a. The Cd(II) removal efficiency was increased by the increase in the adsorbent dosage Fig. 9b. The removal mechanisms of contaminating metal ions by layered double hydroxides participated, isomorphic substitution, surface complexation, chelation and precipitation as reported by Liang et al. [127]. Komarneni et al. were proposed that the mechanism of transition metal ion uptake by MgAl-LDHs was diadochy [128]. Park et al. showed that LDHs eliminated cupper (II) and lead (II) ions from water phase mostly by the precipitation and surface adsorption [129]. The magnetic Fe_3O_4/MgAl-LDHs can be rapidly and simply alienated utilizing a magnet before and after the removal of heavy metals from aqueous solution in adsorption process. There are many hydroxyl groups bonded to octahedral metal atoms on the surface of LDHs and many excess hydroxide ions around the LDHs due to its high buffering capacity. Consequently, the preferred adsorption mechanisms between Mg–Al–CO_3 or Fe_3O_4/Mg–Al–CO_3 LDHs and Cd(II) many include (i) surface adsorption due to the nature of cations (ii) formation of $CdCO_3$ precipitation by anion exchange (iii) formation of outer sphere surface complexes with oppositely charged surface hydroxyl groups. The schematic illustration of the adsorption mechanisms is exposed Fig. 9c.

Drug delivery applications

Fe_3O_4/LDHs nanocomposites is always in the focus of many researchers as of their potential applications in the biomedical field. Between nanomaterials, the iron nanoparticles and two-dimensional layered double hydroxides have great interest in biomedical applications due to their layered structure and unique properties. However, composites of the layered double hydroxide are now budding as potential new drug
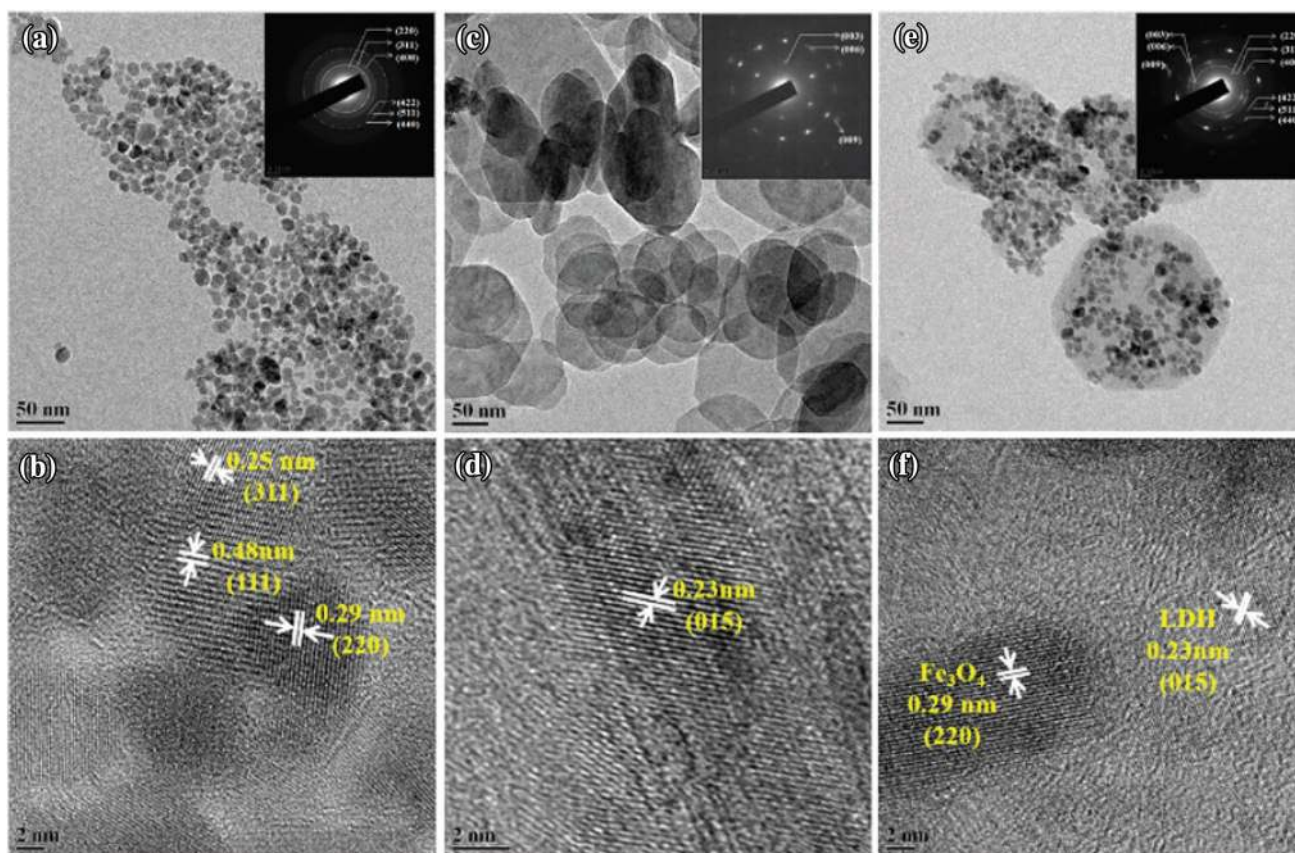

Fig. 10 Transmission electron micrographs along with high resolution micrographs of **a**, **b** Fe_3O_4 nanoparticles, **c**, **d** LDH and **e**, **f** Fe_3O_4/MgAl-LDHs magnetic nanohybrids (insets depict the corresponding SAED patterns) (the figures are adopted and reproduced with permission from Ref. [104])

delivery system due to its low toxicity and advanced biocompatibility [130]. Some studies have shown that the LDHs to have the same or lesser toxicity than the corresponding pure drug it carries when tested on normal cell lines [131]. Application of LDHs for the delivery of non steroidal anti-inflammatory drugs was studied [132]. Many other drugs, such as amino acids, antidiabetic, antioxidants, antibiotics, cardiovascular, and peptides were intercalated into the inorganic nanolayers, which have been widely reviewed recently [133].

Eswara et al. has been studied layered double hydroxide–Fe_3O_4 magnetic nanohybrids for thermo-chemotherapy [104]. Figure 10 shows the electron micrographs of Fe_3O_4 nanoparticles, pure LDH and Fe_3O_4/MgAl-LDHs magnetic nanohybrids with their corresponding selected area electron diffraction (SAED) patterns (inset). Figure 10a demonstrates the Fe_3O_4 nanoparticles with essentially a spherical morphology and narrow size distribution. The particle size was in the range of 10–15 nm. Pure LDHs (Fig. 10c) illustrate a hexagonal morphology with nearly circular edges that have a particle size of 80–100 nm. The SAED patterns that correspond to the diffraction planes of (003), (006) and (009) were indexed. Figure 10e shows Fe_3O_4/MgAl-LDHs magnetic nanohybrids that have Fe_3O_4 nanoparticles that are well decorated and evenly distributed on the LDH surface. The SAED pattern of Fe_3O_4/MgAl-LDHs magnetic nanohybrids demonstrates Fe_3O_4 as the primary phase and the (003) pattern of the LDH phase, which is in agreement with the XRD results. However, the prepared magnetic Fe_3O_4/

MgAl-LDHs composite with to extend the horizons of their applications in cancer therapy. These Fe_3O_4/MgAl-LDHs have been investigated as possible heating platforms for magnetic hyperthermia as well as drug-delivery vectors to cancer cells.

In addition, shang et al. [134] fabricated that the study of poly-(3-thiopheneacetic acid) coated Fe_3O_4@LDHs magnetic nanospheres as a photocatalyst for the photocatalytic disinfection of pathogenic bacteria under solar light irradiation and showed that poly-(3-thiopheneacetic acid) plays a key role in the disinfection process. The OH radicals those are responsible for photocatalytic disinfection can be produced easily from singlet oxygen ($^1O_2$) or superoxide radicals (O_2^-) on the surface of poly-(3-thiopheneacetic acid). So, it was assumed that the photo catalytic disinfection mechanism of this study was owing to the creation of OH, which is created from the surface of Fe_3O_4@PTh-Ac-LDHs. The produced OH could cause significant disorder in the permeability of bacterial cells, DNA damage and decomposition of the cell walls. Furthermore, the outer membrane of the cell was damaged, and the cell was no longer intact leading to leakage of the interior component. This highlights the substantial disorder in membrane permeability by OH in the disinfection process followed by the free efflux of intracellular constituents, which leads to cell death.

More recently, Zhao et al. was utilized core–shell structure of Fe_3O_4@MTX-LDH/Au NPs for cancer therapy [135]. Nearly monodispersed magnetic Fe_3O_4/MTX/LDHs/Au nanoparticles containing the anticancer agent of methotrexate

Fig. 11 Schematic procedure for the preparation of Fe_3O_4@MTX-LDH/Au NPs (the figure is adopted and reproduced with permission from Ref. [135])
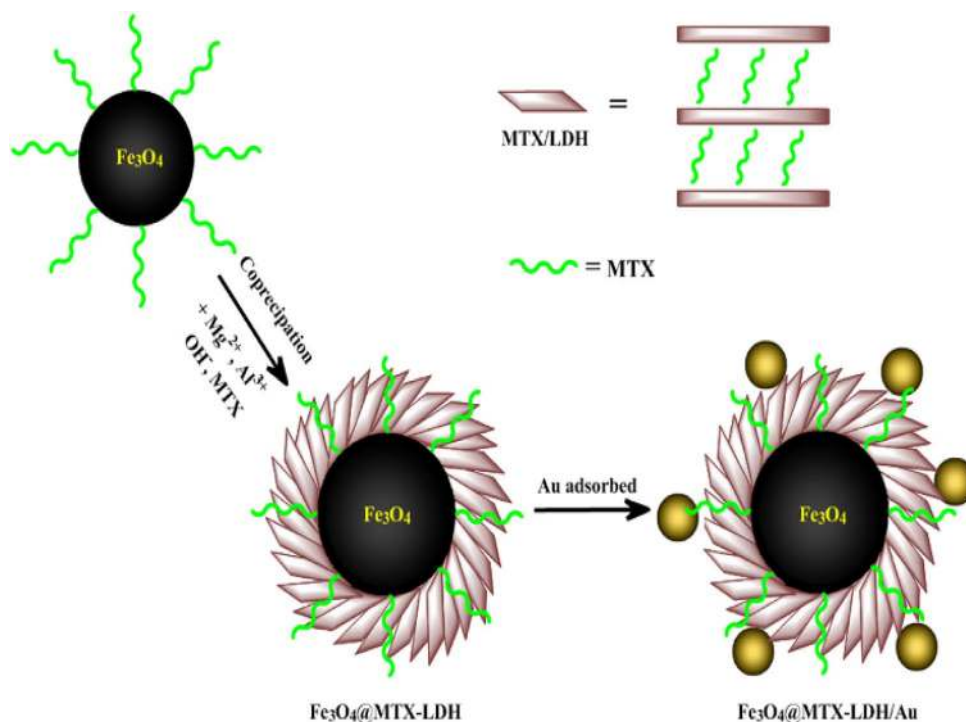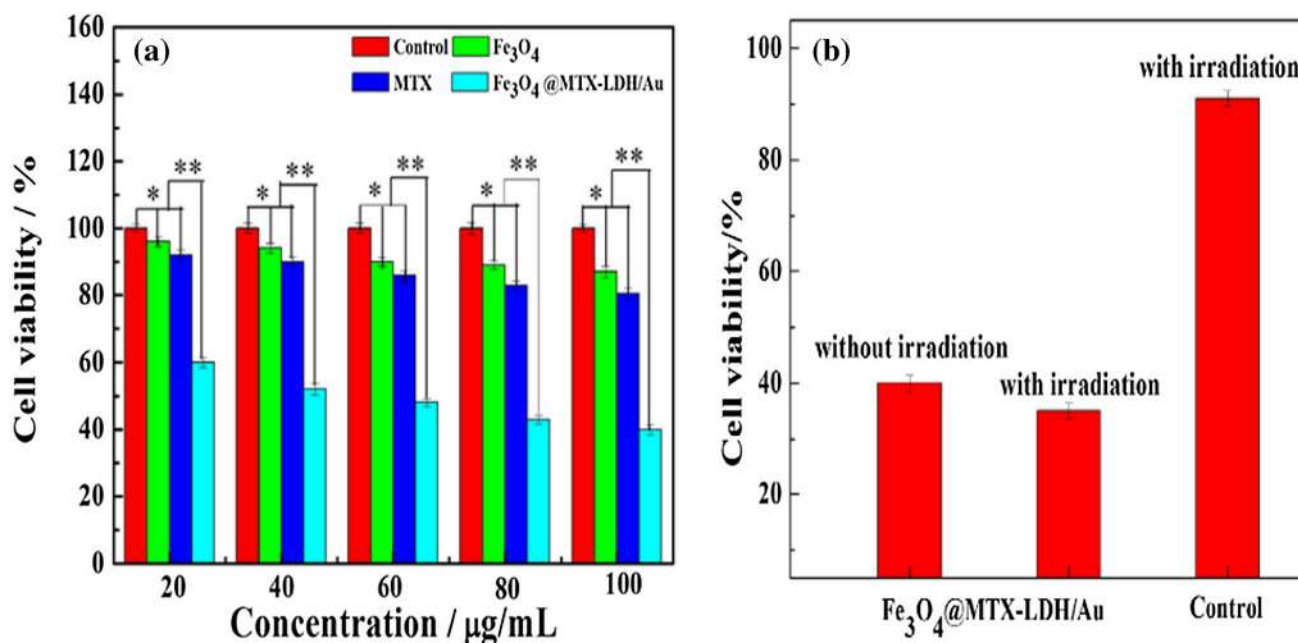
Fig. 12 a Comparison of cell viabilities for MTX, Fe$_3$O$_4$ NPs, Fe$_3$O$_4$@MTXLDH/Au NPs at various concentrations after 48 h of incubation. **b** Comparison of cell viabilities for Fe$_3$O$_4$@MTX-LDH/ Au NPs treated without and with irradiation at the concentration of 100 µg/mL (the figures are adopted and reproduced with permission from Ref. [135])

(MTX) were prepared through co- precipitation electrostatic interaction strategy Fig. 11. Herein, LDHs was used to carry and deliver the anticancer drug of MTX. In this, MTX was used both as the agent for surface modification and the anticancer drug for chemotherapy. Figure 12a exhibited the cell proliferation of MTX, Fe$_3$O$_4$ NPs and Fe$_3$O$_4$@MTX-LDH/ Au NPs calculated at various concentrations after 48 h of incubation. When the concentration increased, the cell viability histogram of MTX and Fe$_3$O$_4$ NPs decreased slowly, while that of Fe$_3$O$_4$@MTX-LDH/Au NPs demonstrated a fast decrease, particularly after long duration. So that confirm the photo thermal therapy ability of Au element, Fe$_3$O$_4$@MTX-LDH/Au NPs at the concentration of 100 µg/ mL were treated with irradiation for 1 h after 47 h of incubation (see Fig. 12b), and the anticancer effect increased extensively after the treatment of irradiation. On the contrary the cell viability was also calculated for the untreated cells but irradiation (named as control sample) and the cell capability was calculated to be 91%. Compared with chemotherapy or photothermal treatment alone, the combined treatment proved a specific synergistic effect, resulting in higher therapeutic efficacy.

Conclusion and perspectives

In summary of recent important articles in the field of magnetic Fe$_3$O$_4$/LDHs nanocomposites, particularly from the viewpoint of the preparation and applications of Fe$_3$O$_4$/ LDHs nano composites for photocatalytic treatment and environmental remediation also discussed. The review highlighted the different preparation methods such solvothermal route, hydrothermal method and co-precipitation method were applied to synthesize the Fe$_3$O$_4$/LDHs nano composites. LDHs correspond to one of the most scientifically promising sample as a result of their lowcost, relative simple synthesis. Magnetic Fe$_3$O$_4$/LDHs nanocomposites are an attractive valuable addition to the field of nanotechnology and are unique materials because of the magnetic nature and more catalytic property compared to the LDHs. The prepared a nano hybrid of Fe$_3$O$_4$ MNPs and layered double hydroxides nano crystals by electrostatic interaction between the two components.

Moreover, magnetic Fe$_3$O$_4$/LDHs nanocomposites are the new promising parts of research particularly in waste water treatment and photocatalysis. The Magnetic Fe$_3$O$_4$/ LDHs nano composites have more surface areas, distinguished adsorption capacity and stability than LDHs. Therefore, these magnetic Fe$_3$O$_4$/LDHs nanocomposites were marked as suitable for water decontamination and photo catalysis purpose; this estimation is only from an academic point of view. In addition, the hazard evaluation

of magnetic Fe_3O_4/LDHs nanocomposites should be explored and their effect on the environmental remediation and photo catalysis studied in a wider context. Up to now magnetic Fe_3O_4/LDHs nanocomposites only were investigated for single pollutant systems. It is extremely suggested to test the presentation of magnetic Fe_3O_4/LDHs nanocomposites in the multi-pollutant polluted water such as organic dyes and toxic metals combined, which will take the research a step additional towards suitable applications.

Compliance with ethical standards

Conflict of interest There are no conflict to declare.

References

1. Prasad, C.H., Murthy, P.K., Krishna, R.H., Rao, R.S., Suneetha, V., Venkateswarlu, P.: Bio-inspired green synthesis of RGO/Fe_3O_4 magnetic nanoparticles using *Murraya koenigii* leaves extract and its application for removal of Pb(II) from aqueous solution. J. Environ. Chem. Eng. **5**, 4374–4380 (2017)

2. Prasad, Ch., Sreenivasulu, K., Gangadhara, S., Venkateswarlu, P.: A facile green synthesis of spherical Fe_3O_4 magnetic nanoparticles and their effect on degradation of methylene blue in aqueous solution. J. Mol. Liq. **221**, 993–998 (2016)

3. Saiah, F.B., Su, B.L., Bettahar, N.: Nickel–iron layered double hydroxide (LDH): textural properties upon hydrothermal treatments and application on dye sorption. J. Hazard. Mater. **165**(1–3), 206–217 (2009)

4. Parida, K.M., Mohapatra, L.: Carbonate intercalated Zn/Fe layered double hydroxide: a novel photocatalyst for the enhanced photo degradation of azo dyes. Chem. Eng. J. **179**, 131–139 (2012)

5. Gautam, R.K., Mudhoo, A., Lofrano, G., Chattopadhyaya, M.C.: Biomass-derived biosorbents for metal ions sequestration: adsorbent modification and activation methods and adsorbent regeneration. J. Environ. Chem. Eng. **2**, 239–259 (2014)

6. Joo, S.H., Faitz, A.J., Sedleck, D.L., Waite, T.D.: Quantification of the oxidizing capacity of nano particulate zero valent iron. Ind. Environ. Sci. Technol. **39**, 1263–1268 (2005)

7. Prasad, Ch., Sreenivasulu, K., Gangadhara, S., Venkateswarlu, P.: Bio inspired green synthesis of Ni/Fe_3O_4 magnetic nanoparticles using *Moringa oleifera* leaves extract: a magnetically recoverable catalyst for organic dye degradation in aqueous solution. J. Alloys Compd. **700**, 252–258 (2017)

8. Shokouhimehr, M., Piao, Y., Kim, J., Jang, Y., Hyeon, T.: A magnetically recyclable nanocomposite catalyst for olefin epoxidation. Angew. Chem. **119**(37), 7169–7173 (2007)

9. Salata, O.V.: Applications of nanoparticles in biology and medicine. J. Nanobiotechnol. **2**, 1–6 (2004)

10. Croce, F., Appetecchi, G.B., Persi, L., Scrosati, B.: Nanocomposite polymer electrolytes for lithium batteries. Nature **394**, 456–458 (1998)

11. Zhao, H., Nagy, K.L.: Dodecyl sulfate-hydrotalcite nanocomposites for trapping chlorinated organic pollutants in water. J. Colloid Interface Sci. **274**(2), 613–624 (2004)

12. Zheng, Y., Zheng, Y., Ning, R.: Effects of nanoparticles SiO_2 on the performance of nanocomposites. Mater. Lett. **57**(19), 2940–2944 (2003)

13. Moniruzzaman, M., Winey, K.I.: Polymer nanocomposites containing carbon nanotubes. Macromolecules **39**(16), 5194–5205 (2006)

14. Prince, J.A., Singh, G., Rana, D., Matsuura, T., Anbharasi, V., Shanmugasundaram, T.S.: Preparation and characterization of highly hydrophobic poly(vinylidene fluoride)–clay nanocomposite nanofiber membranes (PVDF–clay NNMs) for desalination using direct contact membrane distillation. J. Membr. Sci. **397**, 80–86 (2012)

15. Veca, L.M., Meziani, M.J., Wang, W., et al.: Carbon nanosheets for polymeric nano composites with high thermal conductivity. Adv. Mater. **21**(20), 2088–2092 (2009)

16. Shin, S.I., Go, A., Kim, I.Y., Lee, J.M., Lee, Y., Hwang, S.J.: A beneficial role of exfoliated layered metal oxide nano sheets in optimizing the electro catalytic activity and pore structure of Pt-reduced graphene oxide nanocomposites. Energy Environ. Sci. **6**, 608–617 (2013)

17. Lee, J.M., Kim, I.Y., Han, S.Y., Kim, T.W., Hwang, S.J.: Graphene nanosheets as a platform for the 2D ordering of metal oxide nanoparticles: mesoporous 2D aggregate of anatase TiO_2 nanoparticles with improved electrode performance. Chem. Eur. J. **18**(43), 13800–13809 (2012)

18. Paek, S.M., Yoo, E., Honma, I.: Enhanced cyclic performance and lithium storage capacity of SnO_2/graphene nanoporous electrodes with three-dimensionally delaminated flexible structure. Nano Lett. **9**(1), 72–75 (2009)

19. Zhang, F., Song, Y., Song, S., Zhang, R., Hou, W.: Synthesis of magnetite–graphene oxide-layered double hydroxide composites and applications for the removal of Pb(II) and 2, 4-dichlorophenoxyacetic acid from aqueous solutions. ACS Appl. Mater. Interfaces. **7**, 7251–7263 (2015)

20. Hu, B.W., Huang, C.C., Li, X., Sheng, G.D., Li, H., Ren, X.M., Ma, J.Y., Wang, J., Huang, Y.Y.: Marcroscopic and spectroscopic insights into the mutual interaction of grapheme oxide, Cu (II) and Mg/Al layered double hydroxides. Chem. Eng. J. **313**, 527–534 (2017)

21. Ge, X., Gu, C.D., Yin, Z.Y., Wang, X.L., Tu, J.P., Li, J.: Periodic stacking of 2D charged sheets: self-assembled superlattice of Ni–Al layered double hydroxide (LDH) and reduced graphene oxide. Nano Energy. **20**, 185–193 (2016)

22. Li, J., Zhang, N., Ng, D.H.L.: Synthesis of a 3D hierarchical structure of γ-AlO(OH)/Mg–Al–LDH/C and its performance in organic dyes and antibiotics adsorption. J. Mater. Chem. A. **3**, 21106–21115 (2015)

23. Iguchi, S., Teramura, K., Hosokawa, S., Tanaka, T.: Effect of the chloride ion as a hole scavenger on the photocatalytic conversion

of CO_2 in an aqueous solution over Ni–Al layered double hydroxides. Phys. Chem. Chem. Phys. **17**, 17995–18003 (2015)

24. Guo, X.X., Zhang, F.Z., Xu, S.L., Evans, D.G., Duan, X.: Preparation of layered double hydroxide films with different orientations on the opposite sides of a glass substrate by in situ hydrothermal crystallization. Chem. Commun. **44**(28), 6836–6838 (2009)

25. Allmann, R.: The crystal structure of pyroaurite. Acta Crystallogr. Sect. B Struct. Crystallogr. Cryst. Chem. **24**, 972–977 (1968)

26. Taylor, H.F.W.: Segregation and cation-ordering in sjögrenite and pyroaurite. Miner. Mag. **37**, 338–342 (1969)

27. Seftel, E.M., Mertens, M., Cool, P.: LDH and TiO_2/LDH-type nanocomposite systems: a systematic study on structural characteristics. Appl. Catal. B Environ. **134–135**, 274–285 (2013)

28. Seftel, E.M., Popovici, E., Beyers, E., Mertens, M., Zhu, H.Y., Vansant, E.F., Cool, P.: New TiO_2/MgAl-LDH nanocomposites for the photocatalytic degradation of dyes. J. Nanosci. Nanotechnol. **10**, 8227–8233 (2010)

29. Seftel, E.M., Popovici, E., Mertens, M., Stefaniak, E.A., Van Grieken, R., Cool, P., Vansant, E.F.: SnIV-containing layered double hydroxides as precursors for nano-sized ZnO/SnO_2 photocatalysts. Appl. Catal. B Environ. **84**, 699–705 (2008)

30. Yang, X.Y., Zhang, X.Y., Ma, Y.F., Huang, Y., Wang, Y.S., Chen, Y.S.: Superparamagnetic graphene oxide–Fe_3O_4 nanoparticles hybrid for controlled targeted drug carriers. J. Mater. Chem. **19**, 2710 (2009)

31. Cong, H.P., He, J., Lu, Y., Yu, S.H.: Water-soluble magnetic functionalized reduced graphene oxide sheets: in situ synthesis and magnetic resonance imaging applications. Small **6**, 169 (2010)

32. Fu, Y.S., Wang, X.: Magnetically separable $ZnFe_2O_4$–grapheme catalyst and its high photocatalytic performance under visible light irradiation. Ind. Eng. Chem. Res. **50**, 7210 (2011)

33. Tsang, S.C., Caps, V., Paraskevas, I., Chadwick, D., Thompsett, D.: Magnetically separable, carbon-supported nano catalysts for the manufacture of fine chemicals. Angew. Chem. Int. Ed. **43**, 5645 (2004)

34. Elliott, D.W., Zhang, W.X.: Field assessment of nanoscale bimetallic particles for groundwater treatment. Environ. Sci. Technol. **35**, 4922 (2001)

35. Takafuji, M., Ide, S., Ihara, H., Xu, Z.: Preparation of poly(1-vinylimidazole)-grafted magnetic nanoparticles and their application for removal of metal ions. Chem. Mater. **16**, 1977 (2004)

36. Zheng, Y.M., Li, N., Zhang, W.D.: Preparation of nanostructured microspheres of Zn–Mg–Al layered double hydroxides with high adsorption property. Colloids Surf. A Physicochem. Eng. Asp. **415**, 195–201 (2012)

37. Pengcheng, G., Sai, Z., Xing, L., Xiangxue, W., Tao, W., Riffat, J., Ahmed, A., Tasawar, H., Xiangke, W.: Recent advances in layered double hydroxide-based nano materials for the removal of radionuclides from aqueous solution. Environ. Pollut. **240**, 493–505 (2018)

38. Zubair, M., Daud, M., McKay, G., Shehzad, F., Al-Harthi, M.A.: Recent progress in layered double hydroxides (LDH)-containing hybrids as adsorbents for water remediation. Appl. Clay Sci. **143**, 279–292 (2017)

39. Saha, S., Ray, S., Acharya, R., Chatterjee, T.K., Chakraborty, J.: Magnesium, zinc and calcium aluminium layered double hydroxide-drug nanohybrids: a comprehensive study. Appl. Clay Sci. **135**, 493–509 (2017)

40. Sajid, M., Basheer, C.: Layered double hydroxides: emerging sorbent materials for analytical extractions. Trends Anal. Chem. **75**, 174–182 (2016)

41. Mishra, G., Dash, B., Pandey, S.: Layered double hydroxides: a brief review from fundamentals to application as evolving biomaterials. Appl. Clay Sci. **153**, 172–186 (2018)

42. Yang, Z., Wang, F., Zhang, C., Zeng, G., Tan, X., Yu, Z., Zhong, Y., Wang, H., Cui, F.: Utilization of LDH-based materials as potential adsorbents and photocatalysts for the decontamination of dyes wastewater: a review. RSC Adv. **6**, 79415 (2016)

43. Chubar, N., Gilmour, R., Gerda, V., Micusik, M., Omastova, M., Heister, K., Man, P., Fraissard, J., Zaitsev, V.: Layered double hydroxides as the next generation inorganic anion exchangers: synthetic methods versus applicability. Adv. Colloid Interface Sci. **245**, 62–80 (2017)

44. Daud, M., Kamal, M.S., Shehzad, F., Al-Harthi, M.A.: Graphene/layered double hydroxides nanocomposites: a review of recent progress in synthesis and applications. Carbon **104**, 241–252 (2016)

45. Wei, W., He, Q.G., Hong, C.: Surface functionalization and application for magnetic iron oxide nanoparticles. Prog. Chem. **20**, 265–272 (2008)

46. Deng, Y., Qi, D., Deng, C., Zhang, X., Zhao, D.: Superparamagnetic high-magnetization microspheres with an $Fe_3O_4@SiO_2$ core and perpendicularly aligned mesoporous SiO_2 shell for removal of microcystins. J. Am. Chem. Soc. **130**(1), 28–29 (2008)

47. Agrawal, A., Sathe, T., Nie, S.: Single-bead immunoassays using magnetic micro particles and spectral-shifting quantum dots. J. Agric. Food Chem. **55**(10), 3778–3782 (2007)

48. Jia, J., Yu, J.C., Zhu, X.M., Chan, K.M., Wang, Y.X.J.: Ultra fast method to synthesize mesoporous magnetite nanoclusters as highly sensitive magnetic resonance probe. J. Colloid Interface Sci. **379**, 1–7 (2012)

49. Yu, M.K., Jeong, Y.Y., Park, J., Park, S., Kim, J.W., Min, J.J., Kim, K., Jon, S.: Drug-loaded superparamagnetic iron oxide nanoparticles for combined cancer imaging and therapy in vivo. Angew. Chem. Int. Ed. **47**(29), 5362–5365 (2008)

50. Wang, X.L., Zhou, L.Z., Ma, Y.J., Li, X., Gu, H.C.: Control of aggregate size of poly ethyleneimine-coated magnetic nanoparticles for magneto fection. Nano Res. **2**, 365–372 (2009)

51. Hao, B.R., Xing, R., Xu, Z., Hou, Y., Gao, S., Sun, S.: Synthesis, functionalization, and biomedical applications of multifunctional magnetic nanoparticles. Adv. Mater. **22**, 2729–2742 (2010)

52. Ziyuan, X., Yan, C., Zipeng, X., Tianyu, Z., Zhenzi, L., Wei, Z.: Wide spectral response photothermal catalysis-fenton coupling systems with 3D hierarchical $Fe_3O_4/Ag/Bi_2MoO_6$ ternary heterosuperstructural magnetic microspheres for efficient high-toxic organic pollutants removal. J. Colloid Interface Sci. **533**, 24–33 (2019)

53. Luo, Y.L., Fan, L.H., Xu, F., Chen, Y.S., Zhang, C.H., Wei, Q.B.: Synthesis and characterization of Fe_3O_4/PPy/P(MAA-co-AAm) trilayered composite microspheres with electric, magnetic and pH response characteristics. Mater. Chem. Phys. **120**, 590–597 (2010)

54. Sun, S., Murray, C.B., Weller, D., Folks, L., Moser, A.: Monodisperse FePt nanoparticles and ferromagnetic FePt nanocrystal superlattices. Science **287**, 1989–1992 (2000)

55. Jain, T.K., Morales, M.A., Sahoo, S.K., Leslie-Pelecky, D.L., Labhasetwar, V.: Iron oxide nanoparticles for sustained delivery of anticancer agents. Mol. Pharm. **2**, 194–205 (2005)

56. Chourpa, I., Douziech-Eyrolles, L., Ngaboni-Okassa, L., Fouquenet, J.F., Cohen-Jonathan, S., Souce, M., Marchais, H., Dubois, P.: Molecular composition of iron oxide nanoparticles, precursors for magnetic drug targeting, as characterized by confocal Raman microspectroscopy. Analyst **130**, 1395–1403 (2005)

57. Hu, F.X., Neoh, K.G., Kang, E.T.: Synthesis and in vitro anticancer evaluation of tamoxifen-loaded magnetite/PLLA composite nanoparticles. Biomaterials **27**, 5725–5733 (2006)

58. Brijmohan, S.B., Shaw, M.T.: Magnetic ion-exchange nanoparticles and their application in proton exchange membranes. J. Membr. Sci. **303**, 64–71 (2007)

59. Miller, M.M., Prinz, G.A., Cheng, S.F., Bounnak, S.: Detection of a micron-sized magnetic sphere using a ring-shaped anisotropic magnetoresistance-based sensor: a model for a magnetoresistance-based biosensor. Appl. Phys. Lett. **81**, 2211–2213 (2002)

60. Bulte, J.W.: Methods. Intracellular endosomal magnetic labeling of cells. Mol. Med. **124**, 419–439 (2006)

61. Choi, J., Cha, J., Lee, J.K.: Synthesis of various magnetite nanoparticles through simple phase transformation and their shape-dependent magnetic properties. RSC Adv. **3**, 8365–8371 (2013)

62. Shangqing, J., Mingzai, W., Xinxin, Y., Haibo, H., Zhiman, B., Peng, D., Tongtong, J., Hong, B., Guang, L.: RGO/BaFe$_{12}$O$_{19}$/Fe$_3$O$_4$ nanocomposite as microwave absorbent with lamellar structures and improved polarization interfaces. Mater. Res. Bull. **108**, 89–95 (2018)

63. Soto, G.D., Meiorin, C., Actis, D.G., Mendoza Zélis, P., Londoño, O.M., Diego, M., Mosiewicki, M.A., Marcovich, N.E.: Magnetic nanocomposites based on shape memory polyurethanes. Eur. Polym. J. **109**, 8–15 (2018)

64. Unal, B., Durmus, Z., Kavas, H., Baykal, A., Toprak, M.S.: Synthesis, conductivity and dielectric characterization of salicylic acid–Fe$_3$O$_4$ nanocomposite. Mater. Chem. Phys. **123**, 184–190 (2010)

65. Nazrul Islam, M.D., Phong, L.V., Jeong, J.R., Kim, C.G.: A facile route to sono chemical synthesis of magnetic iron oxide (Fe$_3$O$_4$) nanoparticles. Thin Solid Films **519**, 8277–8279 (2011)

66. Deng, Y., Wang, L., Yang, W., Fuselaissari, A.: Preparation of magnetic polymeric particles via inverse microemulsion polymerization process. J. Magn. Magn. Mater. **257**, 69–78 (2003)

67. Franger, S., Berthet, P., Berthon, J.: Electrochemical synthesis of Fe$_3$O$_4$ nanoparticles in alkaline aqueous solutions containing complexing agents. J. Solid State Electrochem. **8**, 218–223 (2004)

68. Luca, D.P., Irene, B., Fabrizio, S., Jacopo, T., Debora, P., Franco, D., Luigi, T.: Synthesis, characterization and performance evaluation of Fe$_3$O$_4$/PES nanocomposite membranes for microbial fuel cell. Eur. Polym. J. **99**, 222–229 (2018)

69. Wu, W., He, Q., Jiang, C.: Magnetic iron oxide nanoparticles: synthesis and surface functionalization strategies. Nanoscale Res. Lett. **3**, 397 (2008)

70. Starowicz, M., Starowicz, P., Żukrowski, J., Przewoźnik, J., Lemański, A., Kapusta, C., Banaś, J.: Electrochemical synthesis of magnetic iron oxide nanoparticles with controlled size. J. Nanopart. Res. **13**, 7167–7176 (2011)

71. Wang, G., Ling, Y., Wheeler, D.A., George, K.E.N., Horsley, K., Heske, C., Zhang, J.Z., Li, Y.: Facile synthesis of highly photoactive α-Fe$_2$O$_3$-based films for water oxidation. Nano Lett. **11**, 3503–3509 (2011)

72. Salazar-Alvarez, G., Muhammed, M., Zagorodni, A.A.: Novel flow injection synthesis of iron oxide nanoparticles with narrow size distribution. Chem. Eng. Sci. **61**, 4625–4633 (2006)

73. Huang, H.Y., Shieh, Y.T., Shih, C.M., Twu, Y.K.: Magnetic chitosan/iron (II, III) oxide nanoparticles prepared by spray-drying. Carbohydr. Polym. **81**, 906–910 (2010)

74. Morjan, I., Alexandrescu, R., Dumitrache, F., Birjega, R., Fleaca, C., Soare, I., Luculescu, C., Filoti, G., Kuncer, V., Vekas, L.: Iron oxide-based nanoparticles with different mean sizes obtained by the laser pyrolysis: structural and magnetic properties. J. Nanosci. Nanotechnol. **10**, 1223–1234 (2010)

75. Martínez, G., Malumbres, A., Mallada, R., Hueso, J., Irusta, S., Bomatí-Miguel, O., Santamaría, J.: Use of a polyol liquid collection medium to obtain ultrasmall magnetic nanoparticles by laser pyrolysis. Nanotechnology **23**, 425605 (2012)

76. Wang, Q., Hare, D.: Recent advances in the synthesis and application of layered double hydroxide (LDH) nanosheets. Chem. Rev. **112**(7), 4124–4155 (2012)

77. Xiaoxiao, G., Fazhi, Z., David, G.E., Xue, D.: Layered double hydroxide films: synthesis, properties and applications. Chem. Commun. **46**, 5197–5210 (2010)

78. Liu, Z., Ma, R., Osada, M., Iyi, N., Ebina, Y., Takada, K., Sasaki, T.: Synthesis, anion exchange, and delamination of Co-Al layered double hydroxide: assembly of the exfoliated nanosheet/polyanion composite films and magneto-optical studies. J. Am. Chem. Soc. **128**, 4872–4880 (2006)

79. Deng, X., Huang, J., Wan, H., Chen, F., Lin, Y., Xu, X., Ma, R., Sasaki, T.: Recent progress in functionalized layered double hydroxides and their application in efficient electrocatalytic water oxidation. J. Energy Chem. (2018). https://doi.org/10.1016/j.jechem.2018.07.007

80. Coronado, E., Galán-Mascarós, J.R., Martí-Gastaldo, C., Ribera, A., Palacios, E., Castro, M., Burriel, R.: Insertion of magnetic bimetallic oxalate complexes into layered double hydroxides. Inorg. Chem. **47**, 9103–9110 (2008)

81. Zhang, C., Tsuboi, T., Namba, H., Einaga, Y., Yamamoto, T.: Enhancement of the coercivity in Co–Ni layered double hydroxides by increasing basal spacing. Dalton Trans. **45**, 13324–13331 (2016)

82. Velu, S., Shah, N., Jyothi, T.M., Sivasanker, S.: Effect of manganese substitution on the physicochemical properties and catalytic toluene oxidation activities of Mg–Al layered double hydroxides. Microporous Mesoporous Mater. **33**, 61–75 (1999)

83. Gu, Z., Atherton, J.J., Xu, Z.P.: Hierarchical layered double hydroxide nano composites: structure, synthesis and applications. Chem. Commun. **51**, 3024–3036 (2015)

84. Xu, Z.P., Zhang, J., Adebajo, M.O., Zhang, H., Zhou, C.H.: Catalytic applications of layered double hydroxides and derivatives. Appl. Clay Sci. **53**, 139–150 (2011)

85. Zhao, M.Q., Zhang, Q., Zhang, W., Huang, J.Q., Zhang, Y.H., Su, D.S., Wei, F.: Embedded high density metal nanoparticles with extraordinary thermal stability derived from guest–host mediated layered double hydroxides. J. Am. Chem. Soc. **132**, 14739–14741 (2010)

86. Yang, Z., Tjiu, W.W., Fan, W., Liu, T.X.: Electrodepositing Ag nanodendrites on layered double hydroxides modified glassy carbon electrode: novel hierarchical structure for hydrogen peroxide detection. Electrochim. Acta **90**, 400–407 (2013)

87. Zhenhua, L., Mingfei, S., Hongli, A., Zixuan, W., Simin, X., Min, W., David, G.E., Xue, D.: Fast electrosynthesis of Fe-containing layered double hydroxide arrays toward highly efficient electrocatalytic oxidation reactions. Chem. Sci. **6**, 6624 (2015)

88. Chen, C., Gunawan, P., Xu, R.: Self-assembled Fe$_3$O$_4$-layered double hydroxide colloidal nanohybrids with excellent performance for treatment of organic dyes in water. J. Mater. Chem. **21**, 1218–1225 (2011)

89. Shao, M., Ning, F., Zhao, J., Wei, M., Evans, D.G., Duan, X.: Preparation of Fe$_3$O$_4$/SiO$_2$/layered double hydroxide core–shell microspheres for magnetic separation of proteins. J. Am. Chem. Soc. **134**, 1071–1077 (2011)

90. Wang, R.X., Wen, T., Wu, X.L., Xu, A.W.: Highly efficient removal of humic acid from aqueous solutions by Mg/Al layered double hydroxides-Fe$_3$O$_4$ nanocomposites. RSC Adv. **4**, 21802–21809 (2014)

91. Lee, C.G., Kim, S.B.: Magnetic alginate-layered double hydroxide composites for phosphate removal. Environ. Technol. **34**, 2749–2756 (2013)

92. Rezvani, Z., Sarkarat, M.: Synthesis and characterization of magnetic composites: intercalation of naproxen into Mg–Al layered double hydroxides coated on Fe$_3$O$_4$. Zeitschrift für anorganische und allgemeine Chemie **638**, 874–880 (2012)

93. Mi, F., Chen, X., Ma, Y., Yin, S., Yuan, F., Zhang, H.: Facile synthesis of hierarchical core–shell Fe_3O_4@MgAl–LDH@Au as magnetically recyclable catalysts for catalytic oxidation of alcohols. Chem. Commun. **47**, 12804–12806 (2011)

94. Pan, D., Zhang, H., Fan, T., Chen, J., Duan, X.: Nearly monodispersed core–shell structural Fe_3O_4@DFUR–LDH sub micro particles for magnetically controlled drug delivery and release. Chem. Commun. **47**, 908–910 (2011)

95. Lu, L., Li, J., Ng, D.H., Yang, P., Song, P., Zuo, M.: Synthesis of novel hierarchically porous Fe_3O_4@MgAl–LDH magnetic microspheres and its superb adsorption properties of dye from water. J. Ind. Eng. Chem. **46**, 315–323 (2017)

96. Mardani, H.R.: (Cu/Ni)–Al layered double hydroxides@Fe_3O_4 as efficient magnetic nano composite photo catalyst for visible-light degradation of methylene blue. Res. Chem. Intermed. **10**, 5795–5810 (2017)

97. Silva, G., Bouizi, Y., Fornes, V., Garcia, H.: Layered double hydroxides as highly efficient photocatalysts for visible light oxygen generation from water. J. Am. Chem. Soc. **131**, 13833–13839 (2009)

98. Parida, K., Satpathy, M., Mohapatra, L.: Incorporation of Fe^{3+} into Mg/Al layered double hydroxide framework effects on textural properties and photocatalytic activity for H_2 generation. J. Mater. Chem. **22**, 7350–7357 (2012)

99. Gao, Y., Wu, J., Zhang, Z., Jin, R., Zhang, X., Yan, X., Umar, A., Guo, Z., Wang, Q.: Synthesis of polypropylene/Mg_3Al-X LDH nanocomposites using a solvent mixing method: thermal and melt rheological properties. J. Mater. Chem. A **1**, 9928–9934 (2013)

100. Koilraj, P., Sasaki, K.: Fe_3O_4/MgAl-NO_3 layered double hydroxide as a magnetically separable sorbent for the remediation of aqueous phosphate. J. Environ. Chem. Eng. **4**(1), 984–991 (2016)

101. Shan, R., Yan, L., Yang, K., Hao, Y., Du, B.: Adsorption of Cd(II) by Mg–Al–CO_3 and magneticFe_3O_4/Mg–Al–CO_3-layered double hydroxides: kinetic, isothermal, thermo dynamic and mechanistic studies. J. Hazard. Mater. **299**, 42–49 (2015)

102. Zhang, H., Zhang, G., Bi, X., Chen, X.: Facile assembly of a hierarchical core@shell Fe_3O_4@CuMgAl-LDH (layered double hydroxide) magnetic nanocatalyst for the hydroxylation of phenol. J. Mater. Chem. A **1**, 5934–5942 (2013)

103. Yan, Q., Zhang, Z., Zhang, Y., Umar, A., Guo, Z., O'Hare, D., Wang, Q.: Hierarchical Fe_3O_4 core–shell layered double hydroxide composites as magnetic adsorbents for anionic dye removal from wastewater. Eur. J. Inorg. Chem. **25**, 4182–4191 (2015)

104. Komarala, E.V.P., Nigam, S., Aslam, M., Bahadur, D.: In-vitro evaluation of layered double hydroxide–Fe_3O_4 magnetic nanohybrids for thermo-chemotherapy. New J. Chem. **40**, 423–433 (2016)

105. Chen, D., Li, Y., Zhang, J., Zhou, J., Guo, Y., Liu, H.: Magnetic Fe_3O_4/ZnCr-layered double hydroxide composite with enhanced adsorption and photo catalytic activity. Chem. Eng. J. **185–186**, 120–126 (2012)

106. Ni, J., Xue, J., Xie, L., Shen, J., He, G., Chen, H.: Construction of magnetically separable NiAl LDH/Fe_3O_4-RGO nanocomposites with enhanced photocatalytic performance under visible light. Phys. Chem. Chem. Phys. **20**, 414–421 (2018)

107. Wang, X., Zhou, S., Wu, L.: Fabrication of Fe^{3+} doped Mg/Al layered double hydroxides and their application in UV lightshielding coatings. J. Mater. Chem. C. **2**, 5752–5758 (2014)

108. Gupta, V.K., Jain, R., Mittal, A., Mathur, M., Sikarwar, S.: Photochemical degradation of the hazardous dye Safranin-T using TiO_2 catalyst. J. Colloid Interface Sci. **309**, 464–469 (2007)

109. Yuan, S., Li, Y., Zhang, Q., Wang, H.: ZnO nanorods decorated calcined Mg–Al layered double hydroxides as photocatalysts with a high adsorptive capacity. Colloids Surf. A **348**, 76–81 (2009)

110. Dvininova, E., Ignata, M., Barvinschib, P., Smithersc, M., Popovicia, E.A.: New SnO_2/MgAl layered double hydroxide composites as photocatalysts for cationic dyes bleaching. J. Hazard. Mater. **177**, 150–158 (2010)

111. Robinson, T., McMullan, G., Marchant, R., Nigam, P.: Remediation of dyes in textile effluent: a critical review on current treatment technologies with a proposed alternative. Bioresour. Technol. **77**, 247–255 (2001)

112. Golob, V., Vinder, A., Simonic, M.: Efficiency of the coagulation/flocculation method for the treatment of dye bath effluents. Dyes Pigments **67**, 93–97 (2005)

113. Papic, S., Koprivanac, N., Bozic, A.L., Metes, A.: Removal of some reactive dyes from synthetic wastewater by combined Al(III) coagulation/carbon adsorption process. Dyes Pigments **62**, 291–298 (2004)

114. Gupta, V.K., Carrott, P.J.M., Ribeiro Carrott, M.M.L.: Suhas.: low cost adsorbents: growing approach to wastewater treatment—a review. Crit. Rev. Environ. Sci. Technol. **39**, 783–842 (2009)

115. Hoffmann, M.R., Martin, S.T., Choi, W., Bahnemann, D.W.: Environmental applications of semiconductor photocatalysis. Chem. Rev. **95**, 69–96 (1995)

116. Tryba, B., Morawski, A.M., Tsumura, T., Toyoda, M., Inagaki, M.: Hybridization of adsorptivity with photocatalytic activity—carbon-coated anatase. J. Photochem. Photobiol. A **167**, 127–135 (2004)

117. Chaara, D., Pavlovic, I., Bruna, F., Ulibarri, M.A., Draoui, K., Barriga, C.: Removalof nitrophenol pesticides from aqueous solutions by layered double hydroxides and their calcined products. Appl. Clay Sci. **50**, 292–298 (2010)

118. Yang, R., Gao, Y., Wang, J., Wang, Q.: Layered double hydroxide (LDH) derived catalysts for simultaneous catalytic removal of soot and NO_x. Dalton Trans. **43**, 10317–10327 (2014)

119. Wu, X.L., Wang, L., Chen, C.L., Xu, A.W., Wang, X.K.: Water-dispersible magnetite-graphene-LDH composites for efficient arsenate removal. J. Mater. Chem. **21**, 17353–17359 (2011)

120. Zhang, X., Wang, J., Li, R., Dai, Q., Gao, R., Liu, Q., Zhang, M.: Preparation of Fe_3O_4@C@layered double hydroxide composite for magnetic separation of uranium. Ind. Eng. Chem. Res. **52**, 10152–10159 (2013)

121. Meinrath, G.: Aquatic chemistry of uranium. Freiberg On-line Geosci. **1**, 101 (1998)

122. Dong, W., Brooks, S.C.: Determination of the formation constants of ternary complexes of uranyl and carbonate with alkaline earth metals (Mg^{2+}, Ca^{2+}, Sr^{2+} and Ba^{2+}) using anion exchange method. Environ. Sci. Technol. **40**, 4689–4695 (2006)

123. Yan, L., Yang, K., Shan, R., Yu, H., Du, B.: Calcined ZnAl- and Fe_3O_4/ZnAl-layered double hydroxides for efficient removal of Cr(VI) from aqueous solution. RSC Adv. **5**, 96495–96503 (2015)

124. Li, Y., Gao, B., Wu, T., Sun, D., Li, X., Wang, B., Lu, F.: Hexavalent chromium removal from aqueous solution by adsorption on aluminum magnesium mixed hydroxide. Water Res. **43**, 3067–3075 (2009)

125. Gwak, G., Kim, M., Oh, J.: Nanocomposites of magnetite and layered double hydroxide for recyclable chromate removal. J. Nanomater. (2016). https://doi.org/10.1155/2016/8032615

126. Li, H., Deng, L., Zhu, G., Kang, L., Liu, Z.H.: Fabrication and capacitance of NiFe LDHs/MnO_2 layered nano composite via an exfoliation/reassembling process. Mater. Sci. Eng. B **177**, 8–13 (2012)

127. Liang, X., Zang, Y., Xu, Y., Tan, X., Hou, W., Wang, L., Sun, Y.: Sorption of metal cations on layered double hydroxides. Colloid Surf. A. **433**, 122–131 (2013)

128. Komarneni, S., Kozai, N., Roy, R.: Novel function for anionic clays: selective transition metal cation uptake diadochy. J. Mater. Chem. **8**, 1329–1331 (1998)

129. Park, M., Choi, C.L., Seo, Y.J., Yeo, S.K., Choi, J., Komarneni, S., Lee, J.H.: Reactions of Cu^{2+} and Pb^{2+} with Mg/Al layered double hydroxide. Appl. Clay Sci. **37**, 143–148 (2007)

130. Kura, A.U., Hussein, M.Z., Fakurazi, S., Arulselvan, P.: Layered double hydroxide nanocomposite for drug delivery systems; biodistribution, toxicity and drug activity enhancement. Chem. Cent. J. **8**, 1–8 (2014)

131. Hussein-Al-Ali, S.H., Al-Qubaisi, M., Hussain, M.Z., Ismail, M., Zainal, Z., Hakim, M.N.: Controlled release and angiotensin-converting enzyme inhibition properties of an antihypertensive drug based on a perindopril erbumine-layered double hydroxide nano composites. Int. J. Nanomed. **7**, 2129–2141 (2012)

132. Rives, V., Arco, M.D., Martin, C.: Layered double hydroxides as drug carriers and for controlled release of non-steroidal anti-inflammatory drugs (NSAIDs): a review. J. Control Release **169**, 28–39 (2013)

133. Rives, V., Arco, M.D., Martin, C.: Intercalation of drugs in layered double hydroxides and their controlled release: a review. Appl. Clay Sci. **88–89**, 239–269 (2014)

134. Shang, K., Sun, B., Sun, J., Li, J., Ai, S.: Poly-(3-thiopheneacetic acid) coated Fe_3O_4@LDHs magnetic nanospheres as a photocatalyst for the efficient photocatalytic disinfection of pathogenic bacteria under solar light irradiation. New J. Chem. **37**, 2509–2514 (2013)

135. Zhao, X., Wang, W.Y., Li, X.D., Li, S., Song, F.: Core-shell structure of Fe_3O_4@MTX-LDH/Au NPs for cancer therapy. Mater. Sci. Eng., C **89**, 422–428 (2018)

136. Wei, Wu, Jiang, C., Vellaisamy, A.L.R.: Recent progress in magnetic iron oxide-semiconductor composite nanomaterials as promising photocatalysts. Nanoscale **7**, 38–58 (2015)

137. Hu, W., Wu, X., Jiao, F., Yang, W., Zhou, Y.: Preparation and characterization of magnetic Fe_3O_4@sulfonated β-cyclodextrin intercalated layered double hydroxides for methylene blue removal. Desalination Water Treat. **57**, 1–12 (2016)

138. Moaser, A.G., Khoshnavazi, R.: Facile synthesis and characterization of Fe_3O_4@MgAl-LDH@STPOM nanocomposite with highly enhanced and selective degradation of methylene blue. New J. Chem. **41**, 9472–9481 (2017)

139. Chen, D., Li, Y., Zhang, J., Li, W., Zhou, J., Shao, L., Qian, G.: Efficient removal of dyes by a novel magnetic Fe_3O_4/ZnCr-layered double hydroxide adsorbent from heavy metal wastewater. J. Hazard. Mater. **243**, 152–160 (2013)

140. Shan, R., Yan, L., Yang, K., Yu, S., Hao, Y., Yu, H., Du, B.: Magnetic Fe_3O_4/MgAl-LDH composite for effective removal of three red dyes from aqueous solution. Chem. Eng. J. **15**, 38–46 (2014)

141. Chen, X., Mi, F., Zhang, H., Zhang, H.: Facile synthesis of a novel magnetic core-shell hierarchical composite submicrospheres Fe_3O_4@CuNiAl-LDH under ambient conditions. Mater. Lett. **69**, 48–51 (2012)

142. Shao, M., Ning, F., Zhao, J., Wei, M., Evans, D.G., Duan, X.: Preparation of Fe_3O_4@SiO_2@layered double hydroxide core–shell microspheres for magnetic separation of proteins. J. Am. Chem. Soc. **134**, 1071–1077 (2012)